3. The $^3T_{1g}$ state is the photoactive state in a number of ligand substitution reactions. The qualitative features of these reactions have been described and rationalized in terms of the ligand field parameters of the original (ground state) molecule.[20] Since the actual parameters of the reacting entity apparently are rather different, one might be tempted to reject this attitude. We are inclined to believe that this is not necessary. Indeed, relaxation is the first step on the dissociative reaction path. By calculating the weakest bond in the initial complex (vertically above the ground state), one determines the most favorable reaction and relaxation coordinates; the course of the photochemical reaction is therefore correctly predicted on the basis of the ground-state parameters.

4. So far, it is not well understood why $Co(NH_3)_6^{3+}$ and its derivatives are characterized by a much lower quantum yield for photosubstitution than $Co(CN)_6^{3-}$ and its derivatives. A possible explanation is found from Figure 2. If a calculation as in Figure 2C is extrapolated for $Co(NH_3)_6^{3+}$, the $^5T_{2g}$ state drops below $^3T_{1g}$ in the expanded molecule! A triplet–quintet crossover takes place in the course of the molecular relaxation. Most molecules follow the energetically favorable quintet path which may not have the properties required for photoreaction; hence the molecule can fall back to the ground state without reaction. Only a few molecules would follow the triplet path and be responsible for the observed quantum yield.

Acknowledgments. Two of the authors (L.V. and J.D.) are indebted to the F.K.F.O. (Fonds voor Kollektief Fundamenteel Onderzoek, Belgium) for financial support.

References and Notes

(1) (a) Laboratory of Inorganic and Analytical Chemistry; (b) Laboratory of Quantum Chemistry.
(2) Z. Stasicka and A. Marchaj, *Coord. Chem. Rev.*, **23**, 131–181 (1977).
(3) R. A. Krause, I. Trabjerg, and C. J. Ballhausen, *Chem. Phys. Lett.*, **3**, 297 (1969).
(4) T. Ohno and S. Kato, *Bull. Chem. Soc. Jpn.*, **43**, 8 (1970); **46**, 1602 (1973).
(5) S. C. Pyke, M. Ogasawara, L. Kevan, and J. F. Endicott, *J. Phys. Chem.*, **82**, 302 (1978).
(6) M. Maestri, F. Bolletta, L. Moggi, V. Balzani, M. S. Henry, and M. Z. Hoffman, *J. Am. Chem. Soc.*, **100**, 2694 (1978).
(7) R. Benasson, C. Salet, and V. Balzani, *J. Am. Chem. Soc.*, **98**, 48 (1976).
(8) A. W. Adamson, M. Larson, and R. Fukuda, results communicated at the VII IUPAC Symposium on Photochemistry, Leuven, July 1978.
(9) M. Mingardi and G. B. Porter, *J. Chem. Phys.*, **44**, 4354 (1966).
(10) K. W. Hipps and G. A. Crosby, *Inorg. Chem.*, **13**, 1543 (1974).
(11) E. Zinato in "Concepts of Inorganic Photochemistry", A. W. Adamson and P. D. Fleischauer, Eds., Wiley-Interscience, New York, 1975, Chapter 4.
(12) G. B. Porter in ref 11, Chapter 2.
(13) Room temperature values in EPA solution are 314 and 260 nm, respectively. Upon cooling to the working temperature the first band shifts to about 308 nm. We assumed a similar UV shift for the second absorption.
(14) J. Fujita and Y. Shimura, *Bull. Chem. Soc. Jpn.*, **36**, 128 (1963).
(15) Barbara Loeb and F. Zuloaga, *J. Phys. Chem.*, **81**, 59 (1977).
(16) The very weak absorption, reported in ref 9, at about 540 nm in the crystalline phase could not be observed.
(17) J. S. Griffith, "The Theory of Transition-Metal Ions", Cambridge University Press, New York, 1971, Appendix 2, Table A29.
(18) M. Gerloch and R. C. Slade, "Ligand Field Parameters", Cambridge University Press, New York, 1973.
(19) J. S. Griffith, "The Irreducible Tensor Method for Molecular Symmetry Groups", Prentice-Hall, Englewood Cliffs, N.J., 1962.
(20) L. G. Vanquickenborne and A. Ceulemans, *J. Am. Chem. Soc.*, **99**, 2208 (1977); **100**, 475 (1978).
(21) K. W. Hipps, G. A. Merrell, G. A. Crosby, *J. Phys. Chem.*, **80**, 2232 (1976).

Intramolecular Hydrolysis of Glycinamide and Glycine Dipeptides Coordinated to Cobalt(III). 2. Reactions of the *cis*-$[Co(en)_2(OH_2/OH)(glyNHR)]^{3+/2+}$ Ions (R = H, $CH_2CO_2C_3H_7$, $CH_2CO_2^-$) and the Effect of Buffer Species

C. J. Boreham, D. A. Buckingham,*† and F. R. Keene†

Contribution from the Research School of Chemistry, Australian National University, Canberra, A.C.T., Australia 2600. *Received April 19, 1978*

Abstract: The intramolecular addition of cobalt(III) bound H_2O and OH^- to glycinamide, glycylglycine isopropyl ester, and glycylglycine also coordinated to Co(III) in the *cis*-$[Co(en)_2(OH_2/OH)(glyNHR)]^{3+/2+}$ ions (R = H, $CH_2CO_2C_3H_7$, $CH_2CO_2^-$) has been investigated both in the absence and presence of buffers. For the dipeptide complex (R = $CH_2CO_2C_3H_7$) both the aqua and hydroxo species form $[Co(en)_2(glyO)]^{2+}$, but loss of hydroxide also occurs resulting in the chelated amide $[Co(en)_2(glyNHR)]^{3+}$. A combination of rate and product analysis data suggests that the initial cyclization is rate determining under all conditions. Buffer species act as general bases in this rate-determining process, but they also enhance the formation of the hydrolysis product. Coordinated water is more reactive than coordinated hydroxide owing largely to a more positive $\Delta S^{\ddagger}$.

In this paper we compare the hydrolysis of glycinamide, glycylglycine, and glycylglycine isopropyl ester coordinated to Co(III) as monodentate ligands to the hydrolysis of the same substrates chelated to Co(III). In the former *cis*-$[Co(en)_2(OH_2/OH)(glyNHR)]^{3+/2+}$ species the amide or dipeptide is attached to the metal through the amino group only, whereas in $[Co(en)_2(glyNHR)]^{3+}$ the oxygen atom of the amide function is also coordinated. The two reactions are schematically represented by Schemes I and II (the oxygen atoms show the fate of hydroxide in the different situations).

^{18}O-Tracer results have established that the coordinated oxygen atom in *cis*-$[Co(en)_2(OH_2/OH)(glyNHR)]^{3+/2+}$ is retained in the hydrolyzed product $[Co(en)_2(glyO)]^{2+}$, and that under alkaline conditions the $[Co(en)_2(glyNHR)]^{3+}$ product also includes the label in the O-bound amide function.[1] These facts require hydrolysis of the monodentate and chelated amide systems **1** and **2** to be interconnected, and in this respect this study bears a close resemblance to the non-metal-catalyzed lactonization of 4-hydroxybutyramides[2,3] and 2-hydroxymethylbenzamides[4,5] where direct intramolecular participation

† Department of Chemistry and Biochemistry, James Cook University of North Queensland, Townsville, Queensland, Australia 4811 (F.R.K.), and Department of Chemistry, University of Otago, P.O. Box 56, Dunedin, New Zealand (D.A.B.).

0002-7863/79/1501-1409$01.00/0 © 1979 American Chemical Society

Scheme I

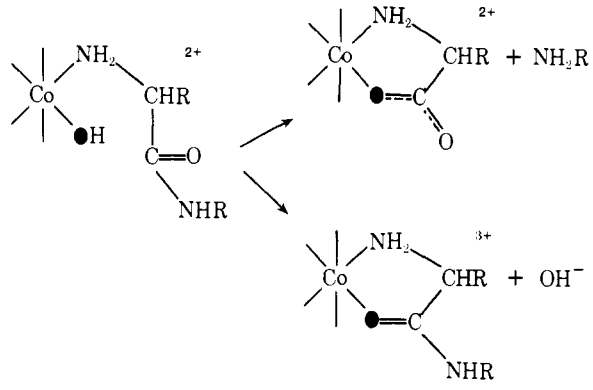

Scheme II

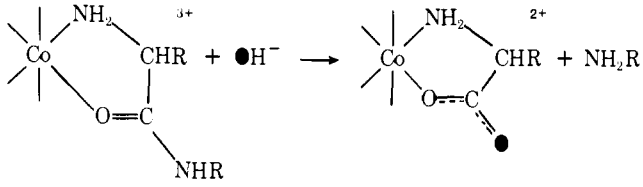

Scheme III

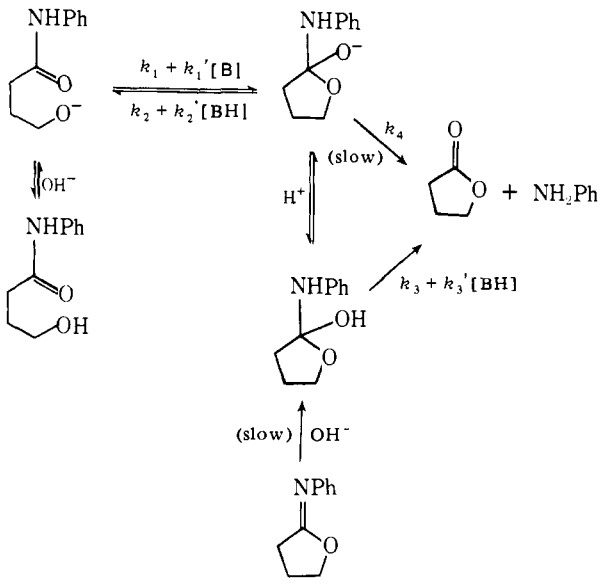

by the hydroxyl group has been suggested. The mechanistic schemes advanced in this latter study are therefore of particular relevance to this report.

For both the aliphatic 4-hydroxybutyranilides[2,3] and the more constrained 2-hydroxymethylbenzamide derivatives[4,5] the rate data in neutral and alkaline solution (pH 5-13) have been interpreted in terms of a change from rate-determining attack of alcoholate anion (k_1, $[OH^-]$ dependent) at pH <8 to rate-determining loss of amine from the neutral (k_3, overall $[OH^-]$ independent) and anionic (k_4, overall $[OH^-]$ dependent) forms of the addition intermediate (Scheme III). Phosphate and carbonate buffers were found to catalyze these processes in slightly alkaline solution (pH ~9), and the nonlinear[5] or asymptotic[3] plots of k_{obsd} vs. [buffer] were interpreted as resulting from a change from rate-determining buffer-catalyzed loss of amine from the neutral intermediate (k_3' [BH]) to cyclization of the alcoholate anion ($k_1'[B]$[5] or k_1,[3] respectively). Parallel studies on the more rapidly hydrolyzing iminolactones[5-7] substantiated this view since the product was diverted from the hydroxy amide to amine plus lactone on addition of buffers.

The chemistry given here closely resembles the above, with i (i.e., *cis*-$[Co(en)_2(OH)(glyNHR)]^{2+}$) being the metal-

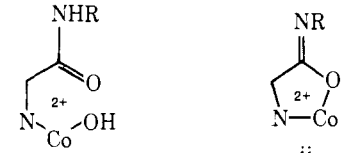

containing analogue of the 4-hydroxy amide and ii (i.e., the conjugate base form of $[Co(en)_2(glyNHR)]^{3+}$) being the metal analogue of the iminolactone. Buffers, particularly bifunctional ones (HPO_4^{2-}, HCO_3^-), also greatly accelerate the metal cyclization reactions, and saturation kinetics are approached under certain conditions. However, the presence of the metal accelerates these processes enormously compared with their organic counterparts, and this and other features have led us to a somewhat different interpretation of the mechanism.

Such differences allow interesting alternatives to the usual role found or anticipated for metal ions in hydrolytic situations.[8,9] Especially the facile intramolecular route for hydrolysis by coordinated water, and the proton tunnelling mechanism used to explain it, have not been described previously. This provides an interesting, and possibly important, alternative to previous schemes advanced for metal-containing hydrolytic enzymes such as carboxypeptidase A.[10,11] It also demonstrates that water (or a hydroxyl function such as a serine residue) in the correct environment can be a very potent nucleophile even though its intrinsic basicity may be low. This has obvious implications for proteolytic enzymes in general.

Experimental Section

Analytical quality reagents were used throughout without further purification. Other materials used are considered in the previous paper.[1] Methyl phosphate and dimethyl phosphate were prepared and recrystallized to analytical purity by the methods of Bunton[12] and Bailly,[13] respectively. Buffer pK_as (μ = 1.0, $NaClO_4$, 25.0 °C) were determined by titration against standard acid or alkali.

Preparation of the *cis*-$[Co(en)_2(OH_2/OH)(glyNHR)]^{3+/2+}$ Ions. For the dipeptide species (R = $CH_2CO_2C_3H_7$, $CH_2CO_2H/CH_2CO_2^-$) the reactant was normally prepared by base hydrolyzing *cis*-$[Co(en)_2Br(glyNHR)]Br_2$ and removing the chelated amide $[Co(en)_2(glyNHR)]^{3+}$ by ion-exchange chromatography at ~2 °C (0.5 M $NaClO_4$, pH 8).[1,14] However, some kinetic runs were carried out on the combined products of base hydrolysis (without ion-exchange separation), and some on the ion-exchange separated product obtained from the reaction with HOCl. Details of these reactions have been given previously.[1] For the glycinamide ions (R = H) kinetic measurements were carried out using the cis species generated by base hydrolysis without ion-exchange removal of $[Co(en)_2(glyNH_2)]^{3+}$. The aquaglycinamide ion reacts too rapidly ($t_{1/2} \simeq 80$ s, 25 °C) to allow it to be used following the HOCl-catalyzed removal of Br.[1]

Product analyses were carried out using the ion-exchange purified reactants (R = $CH_2CO_2C_3H_7$, H). This contains ~9% *trans*-$[Co(en)_2(OH)(glyNHR)]^{2+}$ and allowance is made for this in the results.

Other Preparations 1. $[Co(en)_2(glyglyOC_3H_7)](NO_3)_3$. *cis*-$[Co(en)_2Br(glyglyOC_3H_7)]Br_2 \cdot H_2O$ (7.55 g) and $AgClO_4$ (8.05 g) were shaken for 2 h in acetone (250 mL), AgBr was removed, and the filtrate was taken to dryness. The crude product was purified using ion-exchange chromatography (SP- Sephadex C-25 resin). Unreacted starting material was removed using 0.2 M $NaClO_4$, and the orange 3+ product recovered using 0.5 M pyridinium acetate. The eluate (ca. 2 L) was reduced to dryness and the residue dissolved in H_2O and passed through anion exchange resin (DEAE-Sephadex A-25, NO_3^- form). The eluate volume was reduced to ca. 30 mL, $LiNO_3$ and MeOH were added until crystallization commenced, and the solution was added to well-stirred 2-propanol (750 mL). The orange-yellow precipitate was washed with 2-propanol and ether and dried under

Table II. pK_a and Rate Constants for the Unbuffered Reactions of *cis*-[Co(en)$_2$(OH$_2$/OH)(glyNHR)]$^{3+/2+}$ at 25.0 °C, μ = 1.0 (NaClO$_4$)

complex (R)		pK_a[a]	k_H,[b] s^{-1}	k'_{OH},[b] s^{-1}	k_{OH},[b] M^{-1} s^{-1}
H		6.15 ± 0.1	9.2×10^{-3}	1.5×10^{-4}	2.0
	(20 °C)	6.1 ± 0.1	5.8×10^{-3}	1.1×10^{-4}	1.6
	(30.5 °C)	6.0	1.64×10^{-2}	2.2×10^{-4}	2.8
	(36 °C)	5.8	3.0×10^{-2}	3.45×10^{-4}	3.9
	(25 °C, in D$_2$O)	6.6	8.25×10^{-3} [c]	1.21×10^{-4} [c]	
CH_2CO_2H		2.9[d]	3.3×10^{-4}		
$CH_2CO_2^-$		6.1	7.9×10^{-4}	7.9×10^{-5}	4.5×10^{-2}
$CH_2CO_2C_3H_7$		6.02	3.3×10^{-4}	4×10^{-5}	0.18
	(25 °C, in D$_2$O)		3.07×10^{-4} [c]		

[a] Acidity constant for [Co(en)$_2$(OH$_2$)(glyNHR)]$^{3+}$ species, eq 3 of text, 25.0 °C, μ = 1.0 (NaClO$_4$). [b] From computer fit of rate data (Table I, Figures 1-3) to eq 3;[18] pK_w = 13.77 (25 °C), 13.94 (20 °C), 13.58 (30.5 °C), 13.42 (36.5 °C). [c] In D$_2$O. Observed or calculated rate constants (see text) using pK_w = 14.94[48] and pD = pH + 0.4.[16] [d] pK_a for process *cis*-[Co(en)$_2$(OH$_2$)(glyglyOH)]$^{3+}$ ⇌ *cis*-[Co(en)$_2$(OH$_2$)(glyglyO)]$^{2+}$ + H$^+$.

vacuum: yield 3.0 g (45%); ϵ_{487} 98, ϵ_{342} 111; ^{1}H NMR (C_3H_7) 1.08 (doublet) ppm. Anal. Calcd for [Co(en)$_2$(glyglyOC$_3$H$_7$)](NO$_3$)$_3$·H$_2$O: C, 23.7; H, 5.8; N, 22.6. Found: C, 23.7; H, 5.8; N, 22.5.

2. [Co(en)$_2$(glyglyO)](ClO$_4$)$_2$·H$_2$O. AgClO$_4$ (3.2 g) was added to *cis*-[Co(en)$_2$ Br(glyglyOH)]Br$_2$·2H$_2$O (3.0 g) in acetone (100 mL). After 2 h of shaking AgBr was removed and the filtrate reduced to dryness. The product was recrystallized by dissolution in H$_2$O (10 mL) and adding 0.5 M LiOH solution to pH 6, followed by solid LiClO$_4$ and ethanol. The orange product was washed with ethanol and ether and air dried, yield 2.0 g (78%). Anal. Calcd for [Co(en)$_2$(glyglyO)](ClO$_4$)$_2$·H$_2$O: C, 18.2; H, 4.8; N, 15.9. Found: C, 18.3; H, 5.0; N, 15.8.

3. [Co(en)$_2$(glyNH$_2$)](NO$_3$)$_2$(ClO$_4$) was prepared as described previously.[15]

Kinetic Measurements. Solutions of [Co(en)$_2$(OH)(glyNHR)]$^{2+}$ at pH ~8 were adjusted to μ = 1.0 with NaClO$_4$, and the rate data obtained spectrophotometrically (560 nm (hydroxo), 487 (aqua)), and on occasions by acid or base uptake (0.05 M NaOH, 0.05 M HClO$_4$) using a 3.2-cm thermostated cell under pH-stat control fitted to a Cary 16 K spectrophotometer. For runs in the absence of buffer the pH was rapidly brought to the desired value by syringe or titrimeter addition of acid or base and acceptable data were obtained within 15 s of addition. For runs in the presence of buffers, the desired amount of buffer was rapidly added by syringe or pipet; and the pH maintained by pH-stat control during the remainder of the run. For all experiments at pH >6 it was found essential to use nitrogen-saturated solutions under a nitrogen atmosphere since traces of CO_2 were found to cause spurious effects.

For hydrolysis of the [Co(en)$_2$(glyNHR)]$^{3+}$ ions (R = $CH_2CO_2C_3H_7$, H) a weighed amount of the complex was dissolved in 1.0 M NaClO$_4$ or 0.1 M KCl, and rate data were obtained using the pH-stat equipment and Cary 16 spectrophotometer (280-300 nm). Buffers were added as appropriate by syringe injection.

Product Analysis Experiments. For R = $CH_2CO_2C_3H_7$, $CH_2CO_2H/CH_2CO_2^-$, the solutions from the kinetic runs (>6$t_{1/2}$) were quenched to pH ~4 (HOAc) and the products determined spectrophotometrically (487 nm) and by atomic absorption for Co following absorption on, and elution from, Dowex 50Wx2 cation exchange resin (1 M HClO$_4$/1 M NaClO$_4$ (2+ band), 1 M HClO$_4$/3 M NaClO$_4$ (3+ band)). Experiments were also carried out on larger quantities of material obtained following ion-exchange chromatography (SP-Sephadex, 0.5 M NaClO$_4$, pH 8, 2 °C), by directly quenching into acid, base, or phosphate buffer without following the reaction rates. This latter procedure was used for the R = H complex.

pK_a Measurements. pK_a values for the aqua complexes (R = $CH_2CO_2C_3H_7$, $CH_2CO_2^-$) were measured by titrating ~10^{-3} M solutions of the hydroxo complexes (1.0 M NaClO$_4$, pH (initial) ~8) with 0.1 M HClO$_4$ and following the spectral change at 560 nm. The pK_a was taken as the inflection point in the plot of OD vs. pH. For R = H the titration was carried out rapidly (2 min) since the aqua complex is rather reactive ($t_{1/2} \simeq$ 80 s). pK_a values are given in Table II. A similar procedure was used in D$_2$O except that the deuteroxy amide species was not isolated from the combined products of base hydrolysis. pD was estimated using the expression pD = pH + 0.4.[16] The glass electrode was standardized at 25.0 °C against borate (pH 9.18) and phosphate (pH 6.86) buffers.

Results

1. Reactions of the *cis*-[Co(en)$_2$(OH$_2$/OH)(glyNHR)]$^{3+/2+}$ Ions in the Absence of Buffers. It was found essential to use pH-stat methods to control the pH for the uncatalyzed reactions. Spectrophotometric rate data (D_t) for the three complexes were collected at 487 (aqua) and 560 nm (hydroxo) and are given in Table I for 1.0 M NaClO$_4$ and 0.1 M KCl solutions (supplementary data); similar rate data were obtained from the uptake of acid ($[V_H]_t$ pH-stat) resulting from protonation of released NH_3 or glycine isopropyl ester. For the dipeptide ester complex the optically pure (HOCl produced) and racemate ions gave identical data. For the aqua ions under acid conditions (pH <7) subsequent hydrolysis of the chelated amide ion [Co(en)$_2$(glyNHR)]$^{3+}$ formed as one of the products (R = $CH_2CO_2C_3H_7$, $CH_2CO_2H/CH_2CO_2^-$) does not occur in the times involved, but above pH 9 its rate of hydrolysis becomes comparable with, and then exceeds, that of the hydroxo amide. However, at 560 nm this hydrolysis results in only very small OD changes (<0.01) and could be ignored in the kinetic analysis. Plots of log ($D_\infty - D_t$) or log ($[V_H]_\infty - [V_H]_t$) vs. time were linear for at least 3$t_{1/2}$ for most runs and, except for the hydroxoglycinamide complex at high pH (>11), only one process was observed. For R = $CH_2CO_2C_3H_7$, $CH_2CO_2^-$, the data above pH 12 were complicated by the release of some dipeptide and the formation of a decomposition product. This was not investigated further but product analysis experiments showed that in 1 M NaOH this amounted to ~10% of the reaction.

Plots of log k_{obsd} vs. pH are given in Figures 1-3 and clearly show (except for [Co(en)$_2$(OH$_2$)(glyglyOH)]$^{3+}$ in the pH range 2.5-4.0) three regions of reactivity. From pH 0 to 4 the rate is pH independent, from pH 4 to 9 the rate decreases commensurate with ionization of the coordinated water molecule, and at pHs >9 a term first order in [OH$^-$] predominates for the hydroxo amide complex. The overall rate expression takes the form

$$v = k_H[\text{Co(en)}_2(\text{OH}_2)(\text{glyNHR})^{3+}] + k'_{OH}[\text{Co(en)}_2(\text{OH})(\text{glyNHR})^{2+}] + k_{OH}[\text{Co(en)}_2(\text{OH})(\text{glyNHR}^{2+})][\text{OH}^-] \quad (1)$$

and can be expressed

$$k_{obsd} = \frac{K_a[\text{OH}^-]}{K_w + K_a[\text{OH}^-]}\left[\frac{k_H K_w}{K_a[\text{OH}^-]} + k'_{OH} + k_{OH}[\text{OH}^-]\right] \quad (2)$$

where K_w is the dissociation constant for water (13.77, 1.0 M NaClO$_4$, 25 °C)[17] and K_a is the dissociation constant for the aqua complex.

$$[\text{Co(en)}_2(\text{OH}_2)(\text{glyNHR})]^{3+} + \text{H}_2\text{O} \overset{K_a}{\rightleftharpoons} [\text{Co(en)}_2(\text{OH})(\text{glyNHR})]^{2+} + \text{H}_3\text{O}^+ \quad (3)$$

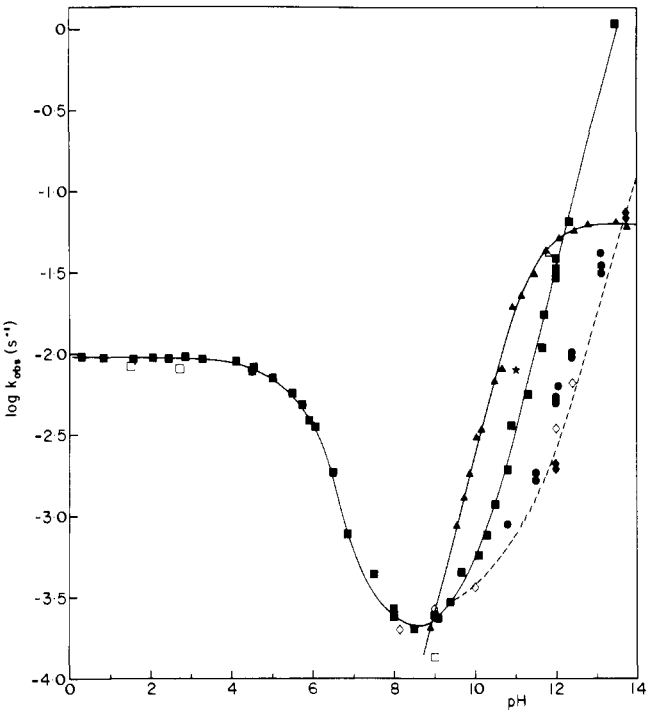

Figure 1. Log k_{obsd} values (■) vs. pH rate profile for the cyclization of *cis*-$[Co(en)_2(OH_2/OH)(glyNH_2)]^{3+/2+}$ at 25.0 °C and μ = 1.0 ($NaClO_4$). The slower reaction of the *trans*-hydroxo ion (- - - - -) observed spectrophotometrically at pH ≥10.8 is given by (●) in 0.1 M KCl and (♦) in 1.0 M KCl. Data for the isolated trans species are given by (◇), 1.0 M $NaClO_4$. Data for the cis ions in D_2O are given by (□), 1.0 M $NaClO_4$. Hydrolysis of the chelated amide $[Co(en)_2(glyNH_2)]^{3+}$ is given by (▲), and the same species obtained from the trans aqua ion by (△); data in D_2O is given by (✱). The solid lines (——) are in each case the best fit calculated curves using the rate expression given by eq 2 and 9, and the constants given in Table II and the text, respectively.

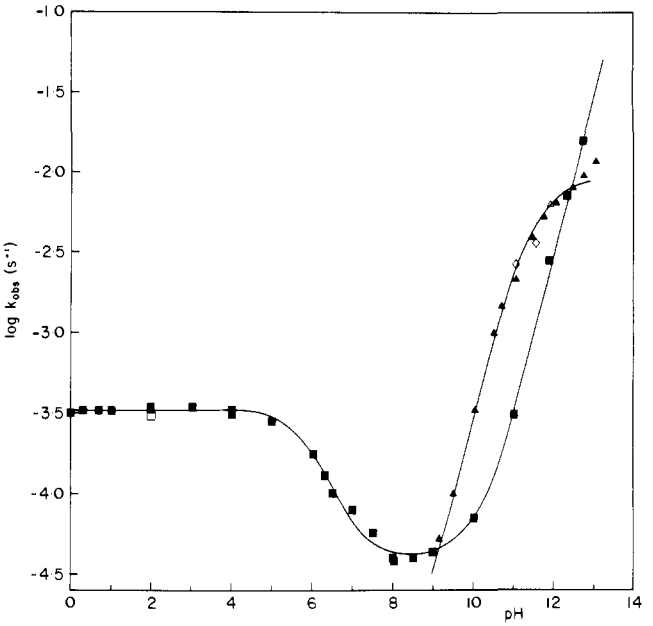

Figure 2. Log k_{obsd} values (■) vs. pH rate profile for the cyclization of *cis*-$[Co(en)_2(OH_2/OH)(glyglyOC_3H_7)]^{3+/2+}$ at 25.0 °C and μ = 1.0 ($NaClO_4$); data in D_2O is given by (□). Hydrolysis data for $[Co(en)_2(glyglyOC_3H_7)]^{3+}$ is given by (▲); the (△) and (◇) data were obtained from the similar ion produced from *trans*-$[Co(en)_2(OH_2)(glyglyOC_3H_7)]^{3+}$ and *trans*-$[Co(en)_2(OH)(glyglyOC_3H_7)]^{2+}$, respectively. The solid lines (——) are the best fit calculated curves obtained using the rate expressions of eq 2 and 9, and the constants given in Table II and the text, respectively.

The rate profile for the glycylglycinate complex (Figure 3) requires the addition of a term of the form $k_H[Co(en)_2(OH_2)(glyglyO)^{2+}]$ to accommodate the enhanced reactivity of the aquaglycylglycinate species (R = $CH_2CO_2^-$). A computer-simulated least-squares fit[18] of the data using separately measured K_a values (Table II) gives the solid curves of Figures 1-3. Values for k_H, k'_{OH}, and k_{OH} are listed in Table II.

Data obtained at 36.5, 30.5, 25.0, and 20.0 °C for $[Co(en)_2(OH_2/OH)(glyNH_2)]^{3+/2+}$ (Table I, μ = 1.0 ($NaClO_4$), supplementary data) resulted in linear Arrhenius plots for each of the three terms of eq 2 giving E_a and $\Delta S^{\ddagger}$ values of 18.3 ± 0.2 kcal mol^{-1} and −8 ± 2 cal deg^{-1} mol^{-1} for k_H, 12.5 ± 0.6 kcal mol^{-1} and −36 ± 4 cal deg^{-1} mol^{-1} for k'_{OH}, and 8.9 ± 0.3 kcal mol^{-1} and −32 ± 2 cal deg^{-1} mol^{-1} for k_{OH}. The last E_a value takes into account $\Delta H°$ for dissociation of H_2O.

Rate data in D_2O for $[Co(en)_2(OH_2)(glyNH_2)]^{3+}$ at pH (measured) 1.47 (pD 1.87[49]) and 2.63 (pD 3.03) gave k_{obsd} = 8.40 × 10^{-3} and 8.1 × 10^{-5} s^{-1}, respectively; similar data for $[Co(en)_2(OH_2)(glyglyOC_3H_7)]^{3+}$ at pH 2.0 (pD 2.4) gave k_{obsd} = 3.07 × 10^{-4} s^{-1}. For $[Co(en)_2(OH)(glyNH_2)]^{2+}$ at pH 9.0 (pD 9.4) k_{obsd} = 1.35 × 10^{-4} s^{-1}; under these conditions the aqua amide contributes 10.0% to k_{obsd}, whence k'_{OH} = 1.21 × 10^{-4} s^{-1}. These data (cf. Figure 1) give $k_{H/D}$ values of 1.11 for the aquaglycinamide complex and 1.24 for the hydroxoglycinamide species.

The reaction products are listed in Table III expressed as the ratio of 2+ ion (entirely $[Co(en)_2(glyO)]^{2+}$) to 3+ ion. For the dipeptide species (R = $CH_2CO_2C_3H_7$, CH_2CO_2H/$CH_2CO_2^-$) the 3+ ion is largely $[Co(en)_2(glyNHR)]^{3+}$ but contains 9 ± 1% *trans*-$[Co(en)_2(H_2O)(glyglyOR)]^{3+}$ for the reactions at pH 1-4; at pH 8 the 3+ product is entirely the chelated dipeptide but some 6% of it derives from the *trans*-hydroxo ion, the remaining 3% of the trans species being hydrolyzed to $[Co(en)_2(glyO)]^{2+}$. For the glycinamide ions (R = H) the 5-8% 3+ product is, or derives from, *trans*-$[Co(en)_2(OH_2)(glyNH_2)]^{3+}$ (pH 1.4) and, although the 3+ ion produced at pH 8 is $[Co(en)_2(glyNH_2)]^{3+}$, it similarly derives (6%) from the *trans*-hydroxo species. Thus the cis aqua- and hydroxoglycinamide ions produce very little or no chelated amide product under conditions where k_H and k'_{OH} control the rate (eq 2). The corresponding cis dipeptide ions form

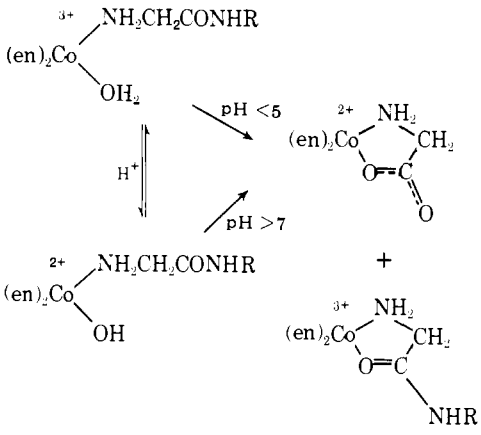

appreciable amounts of the chelated dipeptide species (≃50% for R = $CH_2CO_2C_3H_7$, ≃17% for R = $CH_2CO_2^-$) with the product ratio being little affected by pH. For R = CH_2CO_2H the aqua complex forms more chelated dipeptide (~50%) than the similar complex containing the carboxylate anion. At pH ~9 hydrolysis of $[Co(en)_2(glyNHR)]^{3+}$ becomes competitive with and then exceeds that for the hydroxo amide ion. This is shown in Figures 1-3 with k_{obsd} for the chelated amide being ~ten times that for the hydroxo amide between pH ~10 and 13. This prevents determination of the immediate reaction

Table III. Products of the Unbuffered (pH-Stat) Reactions of the [Co(en)$_2$(OH$_2$/OH)(glyNHR)]$^{3+/2+}$ Ions[a] as a Function of pH (25.0 °C, μ = 1.0 ($NaClO_4$)), Expressed as the Ratio [2+]/[3+][b]

R	pH and [2+]/[3+] ratio							
H	pH 1.0, 95/5			4.0, 94/6, 92/8			8.0[d] 90/10, 89/11	
$CH_2CO_2H/CH_2CO_2^-$ [c]	pH 0.3, 37/63	2.0, 52/48	3.0, 65/35	4.0, 77/23	5.0, 76/24	6.0, 75/25	7.0, 75/25	8.0,[d] 76/24
$CH_2CO_2C_3H_7$	pH 1.0, 46/54		3.0, 44/56	4.0, 43/57	5.0, 43/57		8.0,[d] 39/61, 40/60	

[a] Produced via base hydrolysis of the bromo complex. [b] The 2+ ion is in all cases [Co(en)$_2$(glyO)]$^{2+}$. For R = $CH_2CO_2C_3H_7$, $CH_2CO_2H/CH_2CO_2^-$ the 3+ ion is largely [Co(en)$_2$(glyglyOR)]$^{3+}$ but contains ~6% *trans*-[Co(en)$_2$(OH$_2$)(glyglyOR)]$^{3+}$ (pHs 1–4). For R = H the 3+ ion is, or derives entirely from, *trans*-[Co(en)$_2$(OH$_2$/OH)(glyNH$_2$)]$^{3+/2+}$. [c] pK_a = 2.9. [d] The ratio for the experiment at pH 8.0 is corrected for hydrolysis of the 3+ ion (to 2+) using data given in Figures 1–3.

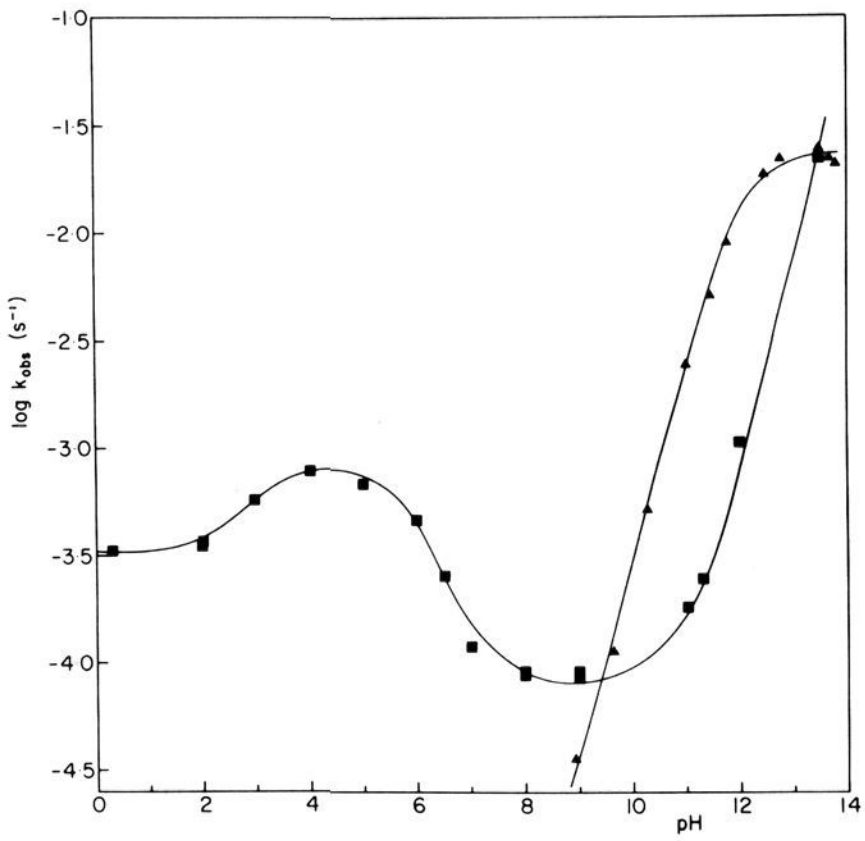

Figure 3. Log k_{obsd} values (■) vs. p*H* rate profile for the cyclization of *cis*-[Co(en)$_2$(OH$_2$/OH)(glyglyOH/glyglyO$^-$)]$^{3+/2+/1+}$ at 25.0 °C and μ = 1.0 ($NaClO_4$). Hydrolysis data for [Co(en)$_2$(glyglyO$^-$)]$^{2+}$ are given by (▲). The solid lines (——) are best fit calculated curves obtained using the rate expressions given by eq 2 and 9, and constants given in Table II and the text, respectively.

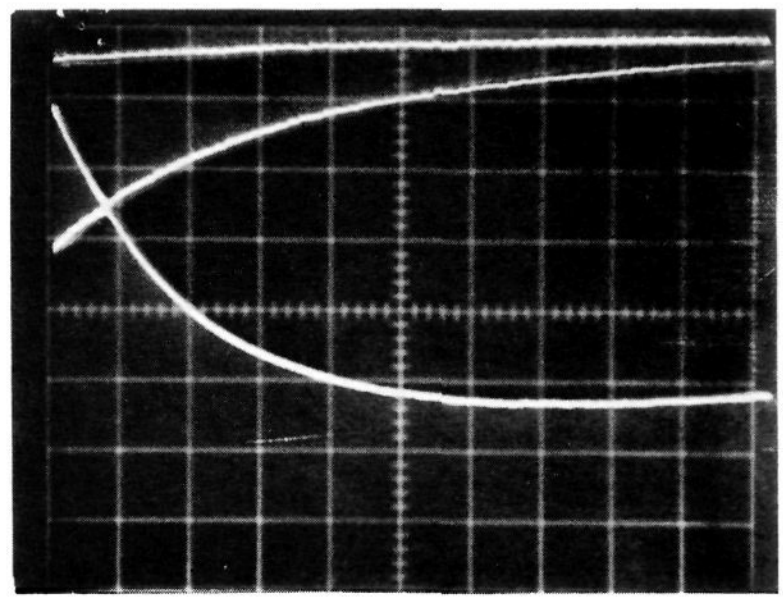

Figure 4. Stopped-flow trace of the change in OD at 560 nm for the reactants of [Co(en)$_2$(OH)(glyNH$_2$)]$^{2+}$ (generated by base hydrolysis of (+)$_{589}$[Co(en)$_2$Br(glyNH$_2$)]Br$_2$ in 0.5 M NaOH, 0.5 M KCl at 25.0 °C. The OD decreases (ordinate down) on time scale (abscissa) of 0.5 s/division, and the slower OD increase is at 5 s/division. Absorption range is 0–1.0, slit 0.1, time constant 10 ms.

products for the hydroxo amide when $k_{OH}[OH^-]$ is rate controlling (eq 2).

At pH >11 the spectrophotometric data (560 nm) for the hydroxoglycinamide complex shows two rate processes of which the first (OD decrease) agrees with that found at lower pHs and is consistent with the rate expression given by eq 2. The subsequent slower process involves an OD increase which becomes more pronounced with increasing pH. Figure 1 gives log k_{obsd} data for the process as a function of pH (1 M $NaClO_4$ and 0.1 M KCl) and Figure 4 gives a stopped-flow trace of the two processes in 0.5 M NaOH. Both reactions were observed with optically pure *cis*-(+)$_{589}$-[Co(en)$_2$Br(glyNH$_2$)]$^{2+}$ and they occurred irrespective of whether [Co(en)$_2$(glyNH$_2$)]$^{3+}$ produced in the initial base hydrolysis of bromide was present or had been previously removed by ion-exchange chromatography at 2 °C. Other experiments showed that [Co(en)$_2$(glyO)]$^{2+}$, also present with the hydroxo complex, was not involved; at the conclusion of the second reaction this species is in fact the major product (>95%). Subsequent experiments demonstrated that this "second reaction" was due to the small amount of *trans*-[Co(en)$_2$(OH)(glyNH$_2$)]$^{2+}$ (9%) present in the red 2+ band. The chemistry of this species is dealt with in a preceding paper.[1] The two rate processes were not observed for either hydroxo dipeptide species.

2. Buffer Catalysis. The addition of buffers affects both the rate and products of the reactions of the hydroxo and aqua amides; they are especially effective in alkaline solution where the hydroxo complex is involved. Tables IV–VI (supplementary data) give rate data for the three complexes [Co(en)$_2$(OH$_2$/OH)(glyNHR)]$^{3+/2+}$ (R = H, $CH_2CO_2C_3H_7$, $CH_2CO_2^-$, respectively) in various buffers, and Figure 5 gives the product analysis results for the dipeptide ester complex in acetate buffers.

The data show that the aquaglycinamide and aquadipeptide ester reactions (pH <5) are retarded by selenate (pK_a = 1.0), sulfate (1.0), phosphate (1.72), glycinate (2.42), furoate (3.16), and tartrate (3.4), with the more highly charged SeO_4^{2-} and SO_4^{2-} ions derived from the most acidic buffers being the most effective. Citrate (3.81, 4.91), succinate (5.2), maleate (5.8), and acetate (4.44) appear to catalyze the reaction slightly under conditions where appreciable amounts of the buffer anion and aqua complex are available. For these buffers the data fit the rate expression

$$v = k_H[\text{Co-OH}_2^{3+}] + k_B[\text{Co-OH}_2][B] + k'_{OH}[\text{Co-OH}^{2+}]$$

with

$$k_B = (k_{obsd} - k_{hyd})(K_a + [H^+])/[B][H^+] \qquad (5)$$

where K_a is the dissociation constant of the aqua complex and B is the basic form of the buffer. The reaction of the hydroxoglycinamide is not catalyzed by acetate (Table IV), and citrate at pH 9.5 has a retarding influence. This, and the observation of general base catalysis for other buffer anions in alkaline solution, suggests that the rate law be interpreted in

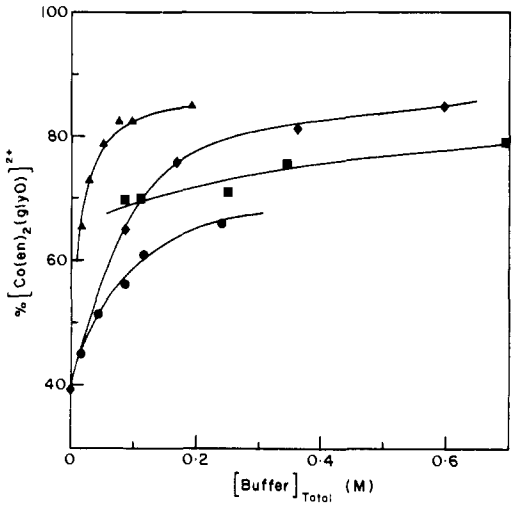

Figure 5. Products of the reaction of $[Co(en)_2(OH_2/OH)(glyglyOC_3H_7)]^{3+/2+}$ in the presence of acetate buffers at pH 4.60 (-♦-♦-♦-), and methyl phosphate buffers at pH 4.0 (-●-●-●), 6.32 (-▲-▲-▲-), and 8.20 (-■-■-■-) expressed as % $[Co(en)_2(glyO)]^{2+}$, the remainder being $[Co(en)_2(glyglyOC_3H_7)]^{3+}$ + 9% *trans*-$[Co(en)_2(OH_2)(OH_2)(glyglyOC_3H_7)]^{3+}$, μ = 1.0 ($NaClO_4$), 25.0 °C.

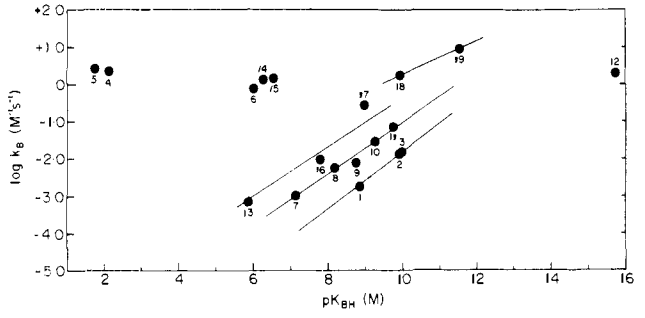

Figure 7. Brønsted plot of log k_B vs. pK_{BH} for the general-base-catalyzed reactions of *cis*-$[Co(en)_2(OH)(glyNH_2)]^{2+}$ at 25.0 ° C and μ = 1.0 ($NaClO_4$): (1) morpholine, (2) 3-quinuclidinol, (3) NEt_3, (4) $HMePO_4^-$, (5) $H_2PO_4^-$, (6) HCO_3^-, (7) *p*-nitrophenol, (8) *m*-nitrophenol, (9) $H_4BO_4^-$, (10) *p*-chlorophenol, (11) phenol, (12) OH^-, (13) $MePO_4^{2-}$, (14) $HAsO_4^-$, (15) HPO_4^{2-}, (16) SeO_3^{2-}, (17) CO_3^{2-}, (18) AsO_4^{3-}, (19) PO_4^{3-}.

terms of general base catalysis of the aqua complex rather than the alternative acid-catalyzed reaction of the hydroxo ions. The reactivity order is ($k_B < 0$, $pK_a < 3.5$) $SeO_4^{2-} \sim SO_4^{2-} < NH_3^+CH_2CO_2^- \sim$ furoate$^- \sim$ tartrate^{2-}; ($k_B > 0$, $pK_a > 4.4$) citrate^{2-} < acetate$^-$ < maleate^{2-} < succinate^{2-}. Product analysis results in the presence of acetate (Figure 5, pH 4.6) show that catalysis promotes the formation of $[Co(en)_2(glyO)]^{2+}$ at the expense of $[Co(en)_2(glyglyO\ C_3H_7)]^{3+}$ with a limiting product composition approaching 87 ± 2% 2+, 13 ± 2% 3+ at $[AcO^-] > 0.6$ M. Much of the 3+ ion derives from the trans aqua complex (see above) but some appears to be produced from the cis species by an acetate-dependent path (~5%).

Marked catalysis of the hydroxo amide reaction occurs with the more basic buffers ($pK_a > 6$), and this has been investigated in detail for $[Co(en)_2(OH)(glyNH_2)]^{2+}$ (Table IV, supplementary data); some data was also collected for the $[Co(en)_2(OH)(glyglyOC_3H_7)]^{2+}$ ion (Table V, supplementary data). For buffers with only a single protonation site (monofunctional buffers) the rate law takes the form

$$k_{obsd} = k'_{OH} + k_{OH}[OH^-] + \frac{k_B K_a[B]}{K_a + [H^+]}$$

Table VII. Second-Order Rate Constants (k_B) for the General-Base-Catalyzed Reactions of the *cis*-$[Co(en)_2(OH_2/OH)(glyNHR)]^{3+/2+}$ Ions (μ = 1.0 ($NaClO_4$), 25.0 °C)

general base B	*cis*-$[Co(en)_2(OH)(glyNH_2)]^{2+}$ 10^3k_B, M^{-1} s^{-1}	*cis*-$[Co(en)_2(OH)(glyglyOC_3H_7)]^{2+}$ 10^3k_B, M^{-1} s^{-1}	
SeO_3^{2-}	9		
p-nitrophenolate	1		
m-nitrophenolate	6		
$H_4BO_4^-$	7.8		
p-chlorophenolate	29		
phenolate	70	3.3	
3-quinuclidinolate	13	0.58	
NMe_3	14		
morpholinate	1.7		
PO_4^{3-}	9100	33[a]	(2)[b]
HPO_4^{2-}	1480	52[a]	(18.5)[b]
$H_2PO_4^-$	2700	120[a]	
$MePO_2^{2-}$	0.64	0.3	
$HMePO_4^-$	2150	81	
CO_3^{2-}	280		
HCO_3^-	730		
AsO_4^{3-}	1670		
$HAsO_4^{2-}$	1310		
$Me_2PO_4^-$	~0	0	
Gly		1.1	
n-$PrNH_2$		~0	
NEt_3		1.7	
Im		~0	
AcO^-	30[a]	2.3	
$Me_2PO_4^-$		~0	
Cit^{3-}		~0	
$HCit^{2-}$	15	~0	
H_2Cit^-	15	~0	
succinate^{2-}		5.3	
maleate^{2-}		4.6	
py		~0	

[a] 2 M $NaClO_4$. [b] Data for R = $CH_2CO_2^-$, μ = 1.0 ($NaClO_4$).

with

$$k_B = (k_{obsd} - k_{hyd})(K_a + [H^+])/K_a[B] \qquad (6)$$

where K_a is the acid dissociation constant of the complex and B is the basic component of the buffer; under conditions of pH well removed from the pK_a, $k_B = (k_{obsd} - k_{hyd})/[B]$. Values of k_{calcd} obtained using the k_B values listed in Table VII are compared with ($k_{obsd} - k_{hyd}$) in Tables IV and V (supplementary data) and it is clear that the basic form of the buffer is involved; Figure 6 (supplementary data) demonstrates this for trimethylamine and phenol. Values of k_B increase with increasing basicity and a plot of log k_B vs. pK_{BH} (Figure 7) shows separate linear correlations for the neutral, 1−, 2−, and 3− bases. The Brønsted slopes are similar for each set, $\beta \simeq 0.7$, consistent with a process involving nonlimiting general base catalysis. With the exception of phosphate and methyl phosphate, buffers of $pK_a < 6$ either retard the reaction (citrate^{3-}, SO_4^{2-}) or have no effect (AcO^-, furoate$^-$), and OH^- seems less effective than might be expected. In order to determine the immediate products of these catalyzed reactions it was necessary to use a buffer, and conditions, where no appreciable hydrolysis of the chelated dipeptide ester product could occur. Phenol (pK_a = 9.74) was chosen, and three experiments under the conditions $k_{obsd} = k_{C_6H_5O}[C_6H_5O^-]$ (1.0, 0.7, and 0.3 M phenolate ion, pH 9.8, μ = 1.0 ($NaClO_4$, 25 °C)) gave 94 ± 3% $[Co(en)_2(glyO)]^{2+}$ with the remainder being the 3+ ion. When it is remembered that some 9% of the reactant is the *trans*-hydroxo amide and that this will be largely unaffected by the conditions it is clear that the buffer diverts the products entirely to $[Co(en)_2(glyO)]^{2+}$. Similar less quantitative results were obtained with other buffers in this series.

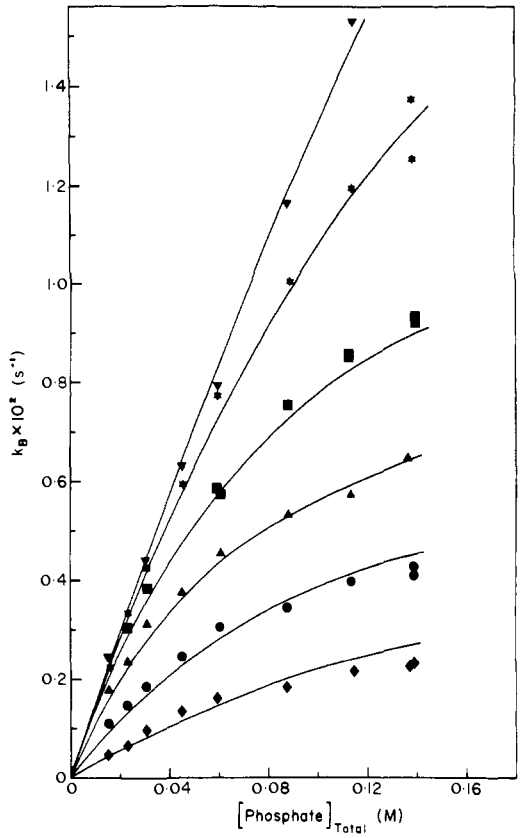

Figure 8. Plot of k_{obsd} vs. [phosphate]$_T$ for the cyclization of $[Co(en)_2(OH)(glyNH_2)]^{2+}$ as a function of pH, 25.0 °C, μ = 1.0 ($NaClO_4$): pH 5.20 (♦), 5.65 (●), 6.15 (▲), 6.70 (■), 7.28 (✱), 7.9 (▼). The solid curves are least squares fitted to eq 8 using $k_{H_2PO_4}$ = 2.7 (0.2), k_{HPO_4} = 1.44 (0.04) M^{-1} s^{-1}, and $K_1 = 2.4 \times 10^{-8}$, $K_2 = 2.06 \times 10^{-6}$ Data at higher pHs are given in Table VII.

For phosphate, methyl phosphate, arsenate, and carbonate, which have more than one basic site, a more complex behavior was observed with both the acidic and basic forms of the buffer contributing to the rate. At pHs well removed from the pK_a of the aqua complex (pH >8.77) the data for $[Co(en)_2(OH)(glyNH_2)]^{2+}$ (Table VIII, supplementary data) and $[Co(en)_2(OH)(glyglyOC_3H_7)]^{2+}$ (Table IX, supplementary data) fit the expression

$$k_{obsd} = k' + k_{OH}[OH^-] + k_B[B] + k_{BH}[BH]$$

or

$$(k_{obsd} - k_{hyd}) = k_B[B] + k_{BH}[BH] \quad (7)$$

However, as the pH approaches the pK_a of the complex, this simple expression fails and a more complex behavior obtains. The data for $[Co(en)_2(OH)(glyNH_2)]^{2+}$ with phosphate and methyl phosphate (Figures 8 and 9, respectively), and for $[Co(en)_2(OH)(glyglyOC_3H_7)]^{2+}$ (Figures 10 and 11, supplementary data) show increasing curvature in the plots of $(k_{obsd} - k_{hyd})$ vs. [phosphate]$_T$ at low pH with a limiting rate being approached in ~0.2 M phosphate when pH $\simeq$ pK_a. The data fits expressions of the form

$$(k_{obsd} - k_{hyd}) = \frac{(k_{H_2PO_4}[H_2PO_4^-] + k_{HPO_4}[HPO_4^{2-}])[OH^-]}{K_1 + [OH^-] + K_2[HPO_4^{2-}]} \quad (8)$$

where $k_{H_2PO_4}$ (k_{HMePO_4}) and k_{HPO_4} (k_{MePO_4}) are rate constants and K_1 and K_2 are ratios of equilibrium constants. The least-squares fitted calculated curves[18] are given as solid lines in the figures ($k_{H_2PO_4}$, k_{HMePO_4}, K_2 fitted) with numerical values for the constants being given in the captions to the figures and in Table VII. It is clear that, whereas $H_2PO_4^{2-}$ and $HMePO_4^{2-}$ have similar catalytic effects, $MePO_4^{2-}$ is very much less effective than HPO_4^{2-}. The significance of this is discussed below.

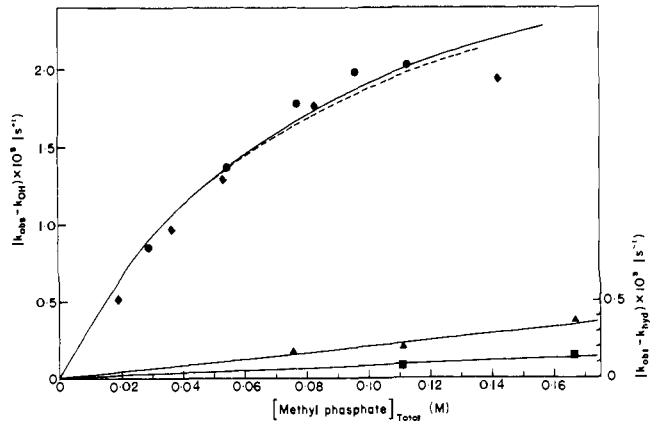

Figure 9. Plot of k_{obsd} vs. [methyl phosphate]$_T$ for the cyclization of *cis*-$[Co(en)_2(OH)(glyNH_2)]^{2+}$ as a function of pH, 25.0 °C, μ = 1.0 ($NaClO_4$): pH 5.74 (♦), 6.3 (●), 9.1 (▲), and 10.1 (■). The solid curves are least squares fitted to eq 8 using k_{MePO_4} = 6.4 × 10^{-4} M^{-1} s^{-1}, k_{HMePO_4} = 2.15 M^{-1} s^{-1}; $K_1 = 2.4 \times 10^{-8}$, $K_2 = 1.06 \times 10^{-6}$.

The deuterium isotope effect was determined at pH 9.35 (pD 9.75)[16] using 0.0185 M phosphate buffer. The k_{obsd} value of 1.75×10^{-2} s^{-1} corresponds to k_{DPO_4} (D_2O) = 0.95 M^{-1} s^{-1}, and when compared with k_{HPO_4} (H_2O) = 1.44 M^{-1} s^{-1} gives k_H/k_D = 1.51.

The products of the phosphate and methyl phosphate catalyzed reactions also differ from those found in the presence of phenol buffers in that both $[Co(en)_2(glyO)]^{2+}$ and $[Co(en)_2(glyglyOC_3H_7)]^{3+}$ are formed. The results for phosphate are given in Figure 12 expressed as % $[Co(en)_2(glyO)]^{2+}$ with the remainder being *trans*-$[Co(en)_2(OH_2)(glyglyOC_3H_7)]^{3+}$ and $[Co(en)_2(glyglyOC_3H_7)]^{3+}$. A limiting composition of 85% $[Co(en)_2(glyO)]^{2+}$ is reached, or approached, under most conditions. Allowing for the 9 ± 1% trans aqua ion present in the initial reactant[1] the limiting composition from the *cis*-hydroxo reactant alone is 94% $[Co(en)_2(glyO)]^{2+}$. That a small amount of $[Co(en)_2(glyglyOC_3H_7)]^{3+}$ is formed by the phosphate-dependent process was confirmed in a separate experiment using $(+)_{589}$-$[Co(en)_2(OH)(glyglyOC_3H_7)]^{2+}$ prepared by base hydrolyzing the optically pure bromo complex.[1] Subsequent reaction at pH 6.64 (40 min) in the presence of 0.15 M phosphate buffer gave a recovered yield of 6.7% trans aqua free $[Co(en)_2(glyglyOC_3H_7)]^{3+}$ with $[M]_{589}$ = +634°. These conditions correspond to saturation formation of $[Co(en)_2(glyO)]^{2+}$ (Figure 12). It was calculated that of the 8.7% *trans*-hydroxo ion present in the initial reactant some 2.5% would have resulted in chelated dipeptide in the time of the experiment.[1] Thus 4.2% of the recovered $[Co(en)_2(glyglyOC_3H_7)]^{3+}$ product derives from the *cis*-hydroxo reactant, and the optical activity for this part ($[M]_{589}$ = +1011°, 62%) corresponds well with that found in the absence of buffers.[1] This suggests that full retention of configuration also obtains in the buffer-catalyzed reaction.

When modified for the trans contaminant and extrapolated to [phosphate]$_T$ = 0 the results of Figure 12 agree with those found in the absence of phosphate (cf. Table X). Finally, attention is drawn to the two other aspects of Figure 12 which will be discussed in detail below. Firstly, the limiting product composition at pH 6.7 is reached at lower phosphate concentrations than at pH 8-9. This suggests that $H_2PO_4^-$ promotes the formation of $[Co(en)_2(glyO)]^{2+}$ more effectively than does HPO_4^{2-} and this is to be contrasted with their similar k_B values

Table X. Products of the Unbuffered Reactions of *cis*-$[Co(en)_2(OH_2/OH)(glyNHR)]^{3+/2+}$ and Unimolecular Rate Constants for Hydrolysis (25 °C, μ = 1.0 ($NaClO_4$))

R	products[a] pH 1-4 (aqua complex)	products[a] pH 8 (hydroxo complex)	rate constant, s^{-1}[b] pH 1-4 (k_H')	rate constant, s^{-1}[b] pH ~9 (k'_{OH})
H	100 ± 2	97 ± 3	9.2×10^{-3}	1.5×10^{-4}
CH_2CO_2H	41 (pH 1)		1.35×10^{-4}	
$CH_2CO_2^-$	83 (pH 4)	80	6.6×10^{-4}	6.3×10^{-5}
$CH_2CO_2C_3H_7$	50 ± 2	41 ± 2	1.65×10^{-4}	1.6×10^{-5}

[a] Expressed as % $[Co(en)_2(glyO)]^{2+}$, the remainder being $[Co(en)_2(glyNHR)]^{3+}$. [b] Calculated rates using product analysis data (Table III).

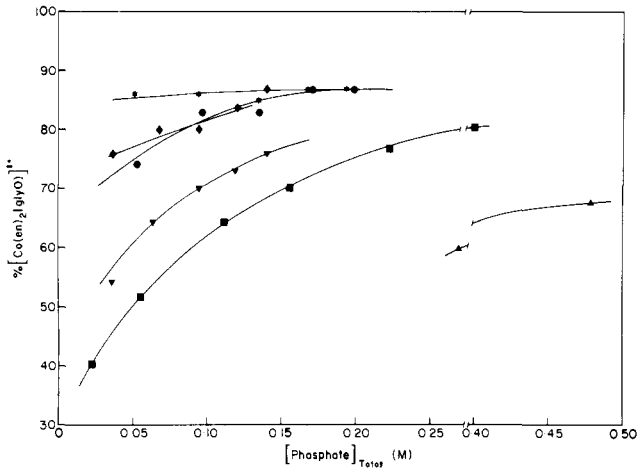

Figure 12. Product composition expressed as % $[Co(en)_2(glyO)]^{2+}$ for the phosphate-catalyzed reaction of $[Co(en)_2(OH)(glyglyOC_3H_7)]^{2+}$, 25.0 °C, μ = 1.0 ($NaClO_4$): 100 − % $[Co(en)_2(glyO)]^{2+}$ represents $[Co(en)_2(glyglyOC_3H_7)]^{3+}$ + 9% *trans*-$[Co(en)_2(OH_2)(glyglyOC_3H_7)]^{3+}$. pH 3.68 (▲), 5.76 (●), 6.64 (✱), 7.15 (♦), 7.71 (▼), 8.77 (■).

(Table VII). Secondly, the product distribution varies under conditions (pH 8.77, for example) where the rate law consists only of the $k_B[HPO_4^{2-}]$ term (eq 7). Thus the products are not decided by the composition of the rate-controlling transition state, and must result from subsequent events with differing phosphate dependencies.

A less detailed set of results for the products of the methyl phosphate catalyzed reaction of the hydroxo dipeptide are given in Figure 5. The data at pH 6.32 demonstrate that $HMePO_4^-$ also promotes the hydrolysis reaction but this again appears not to be exclusive since a limiting composition of 85% 2+, 14% 3+ is reached in 0.2 M buffer corresponding to 94% $[Co(en)_2(glyO)]^{2+}$ and 6% $[Co(en)_2(glyglyOC_3H_7)]^{3+}$ from this cis reactant. The data at pH 8.2 suggest that $MePO_4^{2-}$ either is less discriminatory than $HMePO_4^-$ or does not play as important a part in the formation of products. This is in keeping with its poor catalytic ability in a rate sense (Table VII, Figure 7) when compared with $HMePO_4^-$.

3. Hydrolysis of the Chelated Amide Ions $[Co(en)_2(glyNHR)]^{3+}$. Table XI (supplementary data) contains rate data for hydrolysis of the chelated glycinamide, dipeptide ester, and dipeptide acid complex ions at 25 °C and μ = 1.0 ($NaClO_4$); this is plotted in Figures 1-3, for comparison with the hydroxo monodentate complexes. The temperature dependence for hydrolysis of $[Co(en)_2(glyNH_2)]^{3+}$ gives a linear plot of log k_{obsd} vs. $1/T$, whence E_a = 14.3 ± 0.3 kcal mol^{-1} and $\Delta S^{\ddagger}$ = −7 ± 2 cal deg^{-1} mol^{-1}, and addition of phosphate decreases the rate slightly. For the dipeptide ester complex phosphate buffer has no effect on the rate. For $[Co(en)_2(glyNH_2)]^{3+}$ the observed rate constant in D_2O (1.0 M $NaClO_4$) at pH 11.0 (pD 11.4) was 7.86×10^{-3} s^{-1}; in H_2O at the same OH^- concentration (pH 10.23) k_{obsd} = 3.98 × 10^{-3} s^{-1} (Figure 1). Under these conditions the rate law takes the form $k_{obsd} = k_H[OH^-]$ (see below) giving k_H = 13.8 M^{-1} s^{-1} and k_D = 27.2 M^{-1} s^{-1} with k_H/k_D = 0.51. Similarly in D_2O and 0.1 M KCl, $k_{obsd} = 3.30 \times 10^{-3}$ and 1.15×10^{-2} s^{-1} at pD 10.8 and 11.41, respectively; at the same OH^- concentrations (pH 9.63, 10.24) in H_2O, $k_{obsd} = 1.10 \times 10^{-3}$ s^{-1} and 4.07×10^{-3} s^{-1}, respectively (Figure 1) whence k_H/k_D = 0.39 and 0.35. The conditions used in these experiments preclude significant ionization of the chelated amide moiety (K_b) which ensures that the effects are entirely kinetic in origin.

The plots of log k_{obsd} vs. pH (Figures 1-3) show that below pH ~11 there is a first-order dependence in $[OH^-]$. At higher pHs leveling off in k_{obsd} with increasing $[OH^-]$ occurs, and the data fit the expression[15]

$$k_{obsd} = \frac{k_H K_b [OH^-]}{K_b + [OH^-]} \qquad (9)$$

with k (M^{-1} s^{-1}) and pK_b (M^{-1}) values of 14 ± 1 and 1.4 (R = H), 1.75 ± 0.1 and 1.3 (R = $CH_2CO_2C_3H_7$), and 1.6 ± 0.2 and 1.8 (R = $CH_2CO_2^-$), respectively.[17] The pK_b values have been shown[15] to correspond to ionization of the coordinated amide group (eq 10), and for R = H (Figure 1) and $CH_2CO_2^-$

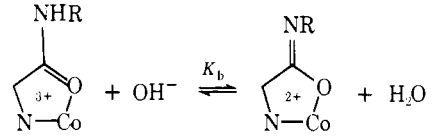

(Figure 3) a limiting rate is clearly observed at pH 13-14. While this is consistent with either solvolysis of the deprotonated amide (H_2O attack) or OH^- attack on the amide, the kinetic solvent isotope ratio (k_H/k_D = 0.3-0.5) clearly favors the latter proposal. Preequilibrium deprotonation usually favors H_2O over D_2O ($K_b(H_2O) > K_b(D_2O)$),[19] and solvolysis of the resulting imide would predict k_H/k_D values of 1.5-5.[20] The alternative mechanism of direct attack of hydroxide would be expected to have k_H/k_D ratios of 0.75,[19] in reasonable agreement with observation.

Figures 1-3 show that hydrolysis of the chelated amide is some ten times faster than the similar unbuffered reactions of the hydroxo amide in the pH range 9-12. However, the rate is little affected by buffers and in this respect it differs considerably from the related intramolecular reaction.

Hydrolysis of $[Co(en)_2(glyNH_2)]^{3+}$ in basic solution (pH 8.5-12) results only in $[Co(en)_2(glyO)]^{2+}$; no hydroxoglycinamide complex, $[Co(en)_2(OH)(glyNH_2)]^{2+}$, was detected either spectrophotometrically or by ion-exchange analysis at 2 °C (SP-Sephadex, 0.5 M $NaClO_4$, pH 8). Similar results hold for hydrolysis of $[Co(en)_2(glyglyOC_3H_7)]^{3+}$ (pH 8.3-12) and in this case the result has special significance since at pH ~ 8 the hydroxo dipeptide has been shown to form ~50% of the chelated dipeptide in the absence of buffer. Figure 13 (supplementary data) gives spectral data for the hydrolysis of $[Co(en)_2(glyglyOC_3H_7)]^{3+}$ at pH 9.14 (Figure 13a) and at pH 8.34 (Figure 13b); under the latter conditions hydrolysis

in the hydroxo ion is some five times faster, and at pH 9.14 their rates are approximately the same (Figure 2). Isosbestic points are maintained (295 nm, pH 9.14), or nearly so (305 nm, pH 8.34), and the data at pH 9.14 and 310 nm gives a linear plot ($4t_{1/2}$) of log ($D_t - D_\infty$) vs. time ($k_{obsd} = 5.35 \times 10^{-5}$ s^{-1}). The hydroxo dipeptide complex shows a large extinction coefficient at these wavelengths (Figure 13b).[1] These results preclude formation of the hydroxo amide in amounts >1% during hydrolysis of the chelated dipeptide. The $[Co(en)_2(glyNHR)]^{3+}$ ions were also shown to be stable over long periods (14 days–3 months) at pHs 1–4.

Discussion

The most significant results are (1) hydrolysis of the monodentate glycinamide and dipeptide occurs by the intramolecular addition of coordinated water or hydroxide; (2) hydrolysis by coordinated water is clearly faster than the unassisted attack by coordinated hydroxide, $k'_H > k'_{OH}$ (Table X); (3) under alkaline conditions competitive hydrolysis (loss of amine) and O-exchange to form the chelated amide (loss of hydroxide) occur with the hydroxo dipeptide complex; under these conditions hydrolysis of the chelated dipeptide fails to open the chelate ring to form the hydroxo amide species; (4) buffers act as general bases and markedly influence the rates for the hydroxo amides, but have little or no effect on the rates for the chelated amides; (5) buffers, and in particular bifunctional ones (e.g., $H_2PO_4^-$), influence the products resulting from the hydroxo amide, with loss of amine being preferred to loss of hydroxide; (6) the uncatalyzed reactions of the aqua and hydroxo amides show no significant kinetic isotope effect ($k_H/k_D = 1.1$) whereas hydrolysis of the chelated amide has a k_H/k_D ratio of 0.3–0.5.

These observations are now considered in some detail.

Hydrolysis in Dilute Acid. The overall reaction in acid solution may be represented as in eq 11, with $k_{obsd} = k_H = k_H'$

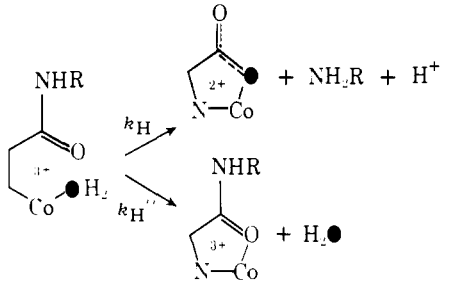

(11)

+ k_H'' (Figures 1–3, Table II). For R = H the reaction is very fast compared to that found in the absence of the metal[21] with $t_{1/2}$ = 75 s, 25.0 °C, and only hydrolysis product results ($k_{obsd} = k_H' = 9.2 \times 10^{-3}$ s^{-1}). For the aqua dipeptide and ester systems only part is hydrolyzed with the product distributions for the cis aqua ions, corrected for that arising from the small amount of trans aqua species, being given in Table X. Thus for R = $CH_2CO_2C_3H_7$ some 50% hydrolysis occurs, with a similar amount (41%) for R = CH_2CO_2H and somewhat more (83%) for the dipeptide anion R = $CH_2CO_2^-$. The ^{18}O-tracer studies for the aqua dipeptide ester system,[1] and for *cis*-$[Co(en)_2(OH_2)(glyNH_2)]^{3+}$,[36] clearly show that the hydrolyzed product contains the coordinated solvent label, with the chelated amide arising from displacement of coordinated water. The similarity in the rates and products for the dipeptide acid system suggests a similar competitive process in this case as well.[22] Most importantly, the ^{18}O results show that the hydrolysis part is completely intramolecular in nature and this requires particularly rapid attack by coordinated water. The values of k_H' given in Table X follow the reactivity order R = H > $CH_2CO_2^-$ > $CH_2CO_2C_3H_7$ ~ CH_2CO_2H, which is that of decreasing basicity of the amine function. This could be

Scheme IV

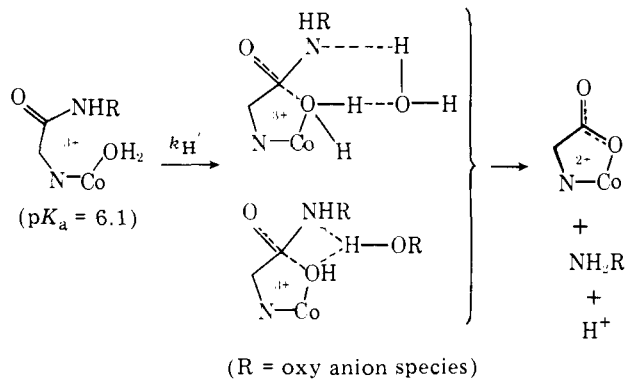

(R = oxy anion species)

interpreted in terms of either rate-controlling addition of water or loss of NH_2R.

The rapidity of the cyclization reaction suggests assistance in the attack of water or in the loss of amine. In view of the inability of water bound to Co(III) to add to easily hydrolyzable substrates in analogous bimolecular reactions ($(NH_3)_5CoOH_2^{3+}$ + CO_2, anhydrides, labile esters,[9] or in intramolecular processes in which a leaving group is not involved[46] (eq 12), we favor a proton tunnelling process (Scheme

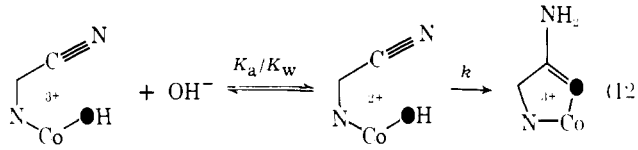

(12)

IV). A similar proposal has been made[25,29] for reactions of metal-aqua species with oxy anions (NO_2^-,[23] SO_3^{2-},[24] IO_3^-,[25] $HAsO_4^{2-}$, $H_2AsO_4^-$,[26] WO_4^{2-} and MoO_4^{2-},[27] CrO_4^{2-},[28] $HSeO_3^-$[29,30]). Leybold stereomodels suggest that transfer to the proton could occur either directly or via the help of an adjacent water molecule, and the moderate amount of catalysis by citrate, succinate, maleate, and acetate clearly supports the latter possibility.

A general base role for acetate with the aqua dipeptide complex is required by eq 5, and production of $[Co(en)_2(glyO)]^{2+}$ is also facilitated (Figure 5). This is consistent with increasing competition by the above intramolecular reaction for the alternative process involving displacement of the coordinated water molecule.[22] Also, these buffer species (H_2O, oxy anions) have basicities intermediate between those of the reactant and the direct addition product iii, and this favors a

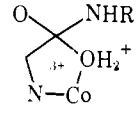

($pK_a \ll 0$)

iii

concerted rather than a stepwise reaction.[31] A similar conclusion follows if the reactant takes the form iv or v and the

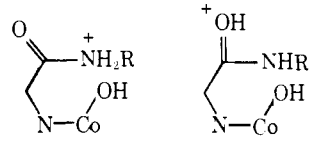

(pK_a (est) < −4)

iv v

addition intermediate vi or vii, but in our view, and in the view of others,[32] it is unnecessary to postulate such high-energy species when lower energy pathways are available.[33]

The lack of an appreciable deuterium isotope effect (k_H/k_D

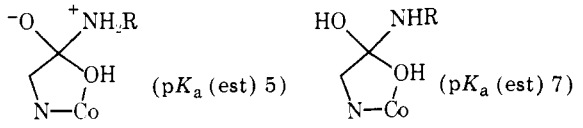

vi vii

= 1.1, Table II) also supports proton tunnelling. It can be argued that the poorer nucleophilic properties of coordinated D_2O (k_H/k_D) > 1) would be offset by the more advanced transfer of D^+ to the departing amine ($k_H/k_D < 1$). In unassisted solvolytic reactions the former secondary isotope effect results in k_H/k_D values of ~2,[20,34] whereas the acid-catalyzed hydrolyses of esters are well-known to have inverse isotope ratios, k_H/k_D = 0.5-0.7.[20] Clearly an intermediate situation applies in Scheme IV with both effects being involved in the transition state.

The retarding influence of some anions (SeO_4^{2-}, SO_4^{2-}, $NH_3^+CH_2CO_2^-$, furoate$^-$, tartrate^{2-}) and the marginal effect of others (citrate$^{2-,3-}$, maleate^{2-}, succinate^{2-}) probably results from substantial ion pairing with the 3+ aqua ion. For HPO_4^{2-}, K_{ip} values of 86 and 54 are found with $[Co(en)_2(OH_2)(glyNH_2)]^{3+}$ and $[Co(en)_2(glyglyOC_3H_7)]^{3+}$ (see below), and similar values were observed by Posey and Taube[35] for the association of SO_4^{2-} with $Co(NH_3)_6^{3+}$. The retarding influence of citrate^{3-} on the rate at pH 9.5 (Table IV) suggests that such ion pairs, in this case 2+/3−, are unreactive or less reactive for buffer species of low basicity. The catalysis observed for acetate at pH 4-5 (Table IV) clearly favors the formation of $[Co(en)_2(glyO)]^{2+}$ (Figure 5, pH 4.6).

Reactions in Neutral and Alkaline Solution. At pH >6 ionization of the coordinated water molecule gives the *cis*-hydroxo amide species, and the physical properties of these ions[1] agree closely with those of *cis*-$[Co(en)_2(OH)NH_3]^{2+}$,[37] which does not have an additional reactive center or deprotonation site under these mild conditions (pH 6-14). Also, the calculated plots of log k vs. pH (Figures 1-3) agree well with the observed data implying that the equilibrium involved in the rate process is indeed the ionization of the bound water molecule. The measured pK_a values used in these calculations were determined by extrapolating the initial spectrophotometric rate data to t = 0 (pH 3-8), and no rapid spectrophotometric process (10 ms) was observed other than the initial (instantaneous) neutralization. Also, in more alkaline solutions, where the $k_{OH}[OH^-]$ term of eq 2 controls k_{obsd} (pH 9-13), no evidence was found for other fast reactions prior to the rate-controlling process. These facts suggest that the observed process involves the hydroxo monodentate amide complex, and that rapid prior cyclization to form an intermediate species is not involved.

The ^{18}O-tracer experiments establish that *both* the hydrolyzed *and* chelated amide products produced from *cis*-$[Co(en)_2(OH)(glyglyOC_3H_7)]^{2+}$ retain the coordinated hydroxyl oxygen for at least the k'_{OH} part of eq 2, and for the k_{HPO_4} part of eq 8. A similar result obtains for the k'_{OH} path

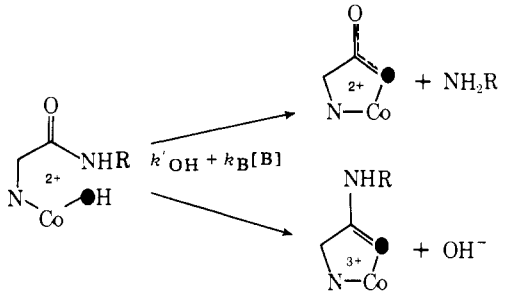

for *cis*-$[Co(en)_2(OH)(glyNH_2)]^{2+}$,[38,39] but the rapid hydrolysis of $[Co(en)_2(glyglyOC_3H_7)]^{3+}$ prevents a direct determination for the $k_{OH}[OH^-]$ part of eq 2 leading to the chelated amide. However, if OH^- behaves as other monofunctional buffers such as phenol (Figure 6) then little chelated amide is likely from this part of the rate law.

Scheme V

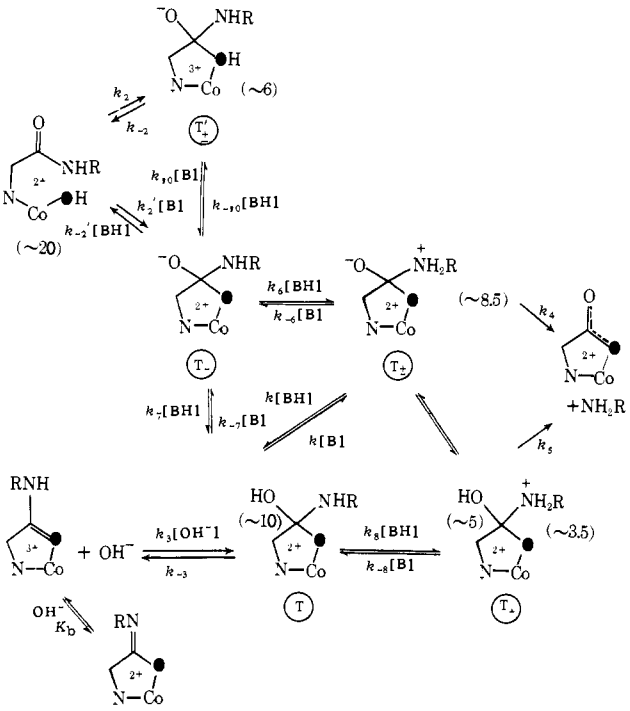

Scheme V details the proposed mechanism for the intramolecular reaction of the hydroxo amide and for hydrolysis of the chelated amide. In this scheme the addition steps k_2, k_2', and k_3 are considered to be rate determining with loss of NH_2R and OH^- occurring as rapid subsequent processes. General base catalysis occurs in the cyclization step ($k_2'[B]$), and the products are believed to result via the common intermediate T. This can decompose by a buffer-independent hydrolysis path to give $[Co(en)_2(glyNHR)]^{3+}$ (k_{-3}), or via buffer-mediated loss of amine (k_4, k_5). The results also require that opening up of the chelate ring (k_{-2}, $k_{-2}[BH]$) is not competitive with retention of the five-membered ring system.

Evidence supporting k_3 and k_2' as the rate-determining steps comes from two main sources. Firstly, the inability of phosphate (or other buffers) to influence the rate of hydrolysis of $[Co(en)_2(glyNHR)]^{3+}$ (the slight retardation observed with PO_4^{3-} for R = H, Table XI, probably results from ion pairing with the 3+ cation) is in marked contrast to the large effect buffer species have on k_2 (represented by $k_2'[B]$) and on the products of the hydroxo amide reaction. Addition of OH^- to the chelated amide forms T directly and, provided that loss of amine requires protonation (either stepwise via T_+ or $T_\pm$, or in a concerted manner without the formation of these intermediates), then the absence of terms in the rate law independent of OH^- (k_5, rate determining) or of the form $k[B]$ (rate-determining formation of T_+) or $k[B][OH^-]$ (rate-determining formation of T_-, or $T_\pm$ for bifunctional buffers) implies that addition of OH^- (k_3) is the rate-determining process for the amide chelate. For the hydroxo dipeptide, the observed variation in the product ratio in the presence of phosphate (e.g., pH 8.77, Figure 12) requires these processes to have different phosphate dependencies where the rate law is entirely of the form $k_{obsd} = k[HPO_4^{2-}]$ (Figure 9). This means that the products are decided by events subsequent to the rate-determining step. This is consistent with rate-determining cyclization to form T_- (monofunctional buffers) or T directly (bifunctional buffers, see below).

The existence of similar intermediates has been established previously and their properties are in general agreement with

those found here. Thus in the aminolysis of the chelated glycine isopropyl ester complex [Co(en)$_2$(glyOC$_3$H$_7$)]$^{3+}$ in non-aqueous solution, the intermediate viii has been observed,[40]

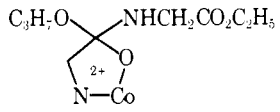

viii

and in neutral to alkaline aqueous conditions (pH >5) it forms largely [Co(en)$_2$(glyNHR)]$^{3+}$; that is, loss of $C_3H_7O^-$ competes favorably with loss of amine. In aqueous acidic solution amine is lost (presumably via T$_+$) with the eventual formation of [Co(en)$_2$(glyO)]$^{2+}$ by subsequent rapid hydrolysis of the chelated ester product. Similarly, hydrolysis of the six-membered ester chelates [Co(en)$_2$(β-alaOC$_3$H$_7$)]$^{3+}$ occurs via rate-determining loss of $C_3H_7O^-$ (or C_3H_7OH) from the neutral and anionic forms of the tetrahedral intermediate, viz.,[41] T and T$_-$. This result differs from that found here for

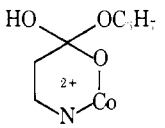

T

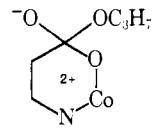

T$_-$

the chelated amide in that $k_3[OH^-]$ is not rate determining for the β-alanine ester complex under conditions where T predominates, and is consistent with the proposal[34] that protonated amine is a better leaving group than an alkoxide ion of similar or greater basicity.

The rate enhancements afforded by the monofunctional buffers show no evidence for a change in the rate-determining step. Thus the Brønsted plots for the neutral amine buffers, and for the 1−, 2−, and 3− oxy anions, are linear (Figure 7), and the individual plots of k_{obsd} vs. [B] (Figure 6) show no curvature at high buffer concentrations. The one exception to the former result is OH^- (Figure 7), but this species may well have an unusual behavior in the aqueous environment and it is not uncommon to find its nucleophilic properties masked compared with its pK_a. The separate correlations for the 1−, 2−, and 3− oxy anions probably result from the overall 2+ charge on the reactant rather than from an inherent difference in catalytic ability. However, ion-pair formation was not observed spectrophotometrically (~300 nm) on addition of buffer, or from deviations in linearity in the plots of k_{obsd} vs. [B].

A concerted rather than stepwise role is envisioned for the buffer species. In this way the less stable (under alkaline conditions) intermediate T$_\pm$′ is avoided, and estimates of 20 and 6 for the pK_as of the hydroxo amide and T$_\pm$′ support a concerted role for most bases including OH^-.[31] However, T$_\pm$′ cannot be avoided for the uncatalyzed reaction (k'_{OH}) and this is probably why this process is comparatively slow. Certainly $\Delta H^\ddagger$ is reduced when the OH^--catalyzed (k_{OH}, $\Delta H^\ddagger$ = 8.3 ± 0.3 kcal mol^{-1}) and uncatalyzed (k'_{OH}, $\Delta H^\ddagger$ = 11.9 ± 0.6 kcal mol^{-1}) reactions are compared. However, the observed k_H/k_D ratios of 1.1 (R = H) and 1.2 (R = $CH_2CO_2C_3H_7$) for the uncatalyzed reaction (k'_{OH}) are unexpected in the absence of solvent involvement in the cyclization process. Coordinated OD^- might be expected to be more nucleophilic than coordinated OH^- if the normal situation obtains.[19]

The remarkable catalysis shown by $H_2PO_4^-$, $HMePO_4^-$, HPO_4^{2-}, HCO_3^-, and $HAsO_4^-$ (Figure 7) must reside in their containing a proton since $MePO_4^{2-}$, AsO_4^-, CO_3^{2-}, and PO_4^{3-} behave normally. The ability of these buffers to donate and accept protons in a concerted manner provides a direct route to T or T$_\pm$ via transition states which resemble that given in Scheme IV for the reaction in acid, viz., eq 13. This concerted general-acid/general-base property will also tend to hold

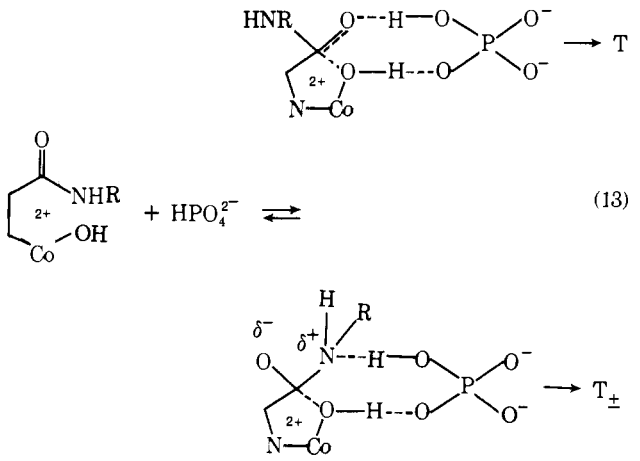

(13)

the two reacting centers together, thereby lowering the configurational free energy component.

The curvature observed at low pHs in the plots of k_{obsd} vs. [phosphate]$_T$ (Figures 8 and 10) and [Mephosphate]$_T$ (Figures 9 and 11) can be accounted for by the formation of unreactive 3+/2− ion pairs between *cis*-[Co(en)$_2$(OH$_2$)(glyNHR)]$^{3+}$

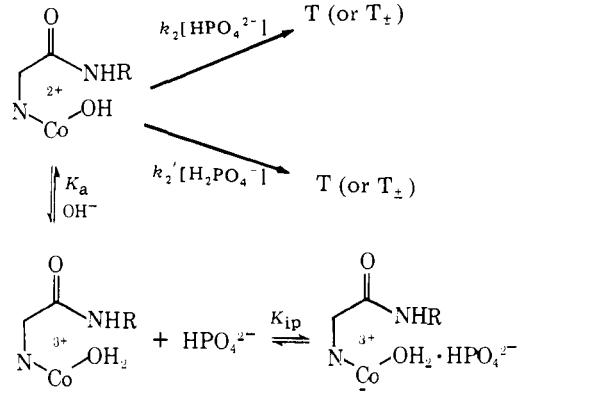

and HPO_4^{2-} or $MePO_4^{2-}$. Similarly SO_4^{2-}, citrate^{2-}, succinate^{2-}, and maleate^{2-} retard the reaction of the aqua amide. The rate constants for $H_2PO_4^-$ and $MeHPO_4^-$ given in Table VII and depicted in the Brønsted plot (Figure 7) assume this mechanism. This process leads to the rate expression

$$k_{calcd} = \frac{K_a[OH^-](k_2[HPO_4^{2-}] + k'_2[H_2PO_4^-])}{K_w + K_a[OH^-] + K_{ip}K_w[HPO_4^{2-}]} \quad (14)$$

which agrees with the observed rate law (eq 8) using K_{ip} values of 86 (10) M^{-1} (R = H) and 54 (10) M^{-1} (R = $CH_2CO_2C_3H_7$) for HPO_4^{2-} and 44 (R = H) and 65 M^{-1} (R = $CH_2CO_2C_3H_7$) for $MePO_4^{2-}$. The solid curves given in Figures 8-11 are for eq 14. K_{ip} values of this magnitude are not unreasonable for 3+/2− ion pairs.[35,42]

Some comment is appropriate on the existence of the intermediates given in Scheme V, and on the estimates for their pK_as.[43] The formation of the chelated amide and chelated acid from the hydroxo dipeptide requires the formation of an intermediate following the rate-determining cyclization process, and the variation in product composition with increasing or changing buffer requires the decay of such an intermediate, or intermediates, to have varying or different buffer dependencies. All three leaving groups (Co-O$^-$, RNH$^-$, and OH$^-$) are poor ones since they are all strong bases. Thus Co-O$^-$ and RNH$^-$ require protonation either prior to or in the act of departure and Co-O$^-$ is almost as poor a leaving group as RNH$^-$. The pK_a values given in parentheses in Scheme VII were estimated[43] according to the procedure of Fox and Jencks,[44] and should be accurate to ~1 pK_a unit. In the absence of buffers this allows the following estimates for the rates of interconversion.

Scheme VII

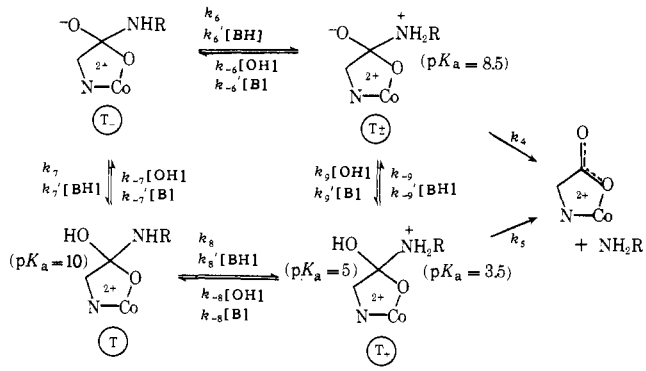

The proton transfers $T_{\pm} \rightarrow T_-$ (k_{-6}), $T_+ \rightarrow T_{\pm}$ (k_9), $T_+ \rightarrow T$ (k_{-8}), and $T \rightarrow T_-$ (k_{-7}) with the strong base OH^- are all thermodynamically favorable and will occur at or close to the diffusion-controlled limit of 10^{10} M^{-1} s^{-1} (i.e., 10^4 s^{-1} at pH 8). The reverse protonations by H_2O ($k_i = k_{-i}K_w/K_b$) will therefore have rates of $\sim 3 \times 10^4$ (k_6), 10 (k_{-9}), 0.3 (k_8), and 10^6 (k_7) s^{-1}. The similar rates for protonation by H_3O^+ (BH) will be diffusion controlled, 5×10^{10} M^{-1} s^{-1}, which at pH 8 will be of the order of 5×10^2 s^{-1}. Loss of protonated amine from $T_{\pm}$ (k_4) will be fast and, if a rate in excess of 10^9 s^{-1} occurs, as has been estimated for other alkylamine intermediates of similar constitution, e.g.,[45] eq 15, then (in the absence of buffer species) the proton transfer steps to form $T_{\pm}$ and T_+ will

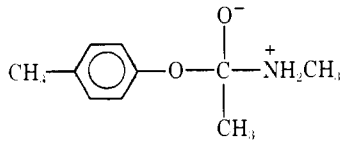

$T_{\pm}$

be the slow steps following the rate-determining formation of T_- and T. Also, since at pH 8 approximately half the product from the hydroxo dipeptide is chelated amide, then k_{-3} will have a value of $\sim 3 \times 10^4$ s^{-1} and the major route to hydrolysis product will be via $T_{\pm}$. Indeed, under these conditions T_+ will not be a major route to hydrolysis product from either the chelated amide or hydroxo amide species and will only begin to contribute at lower pHs. Also $T_{\pm}$, once formed, will prefer to decompose with loss of amine rather than interconvert to T_+ since the latter process will be slow at pH 8 ($k_{-9} = 5 \times 10^2$ s^{-1}). It can also be appreciated why the chelated amide fails to open up the chelate ring and form the hydroxo amide. An estimate of 6 for the pK_a of $T_{\pm}$'[43] (Scheme V) leads to rates for protonation of T_- of $\sim 10^2$ s^{-1} for both the H_3O^+ (at pH 8) and H_2O paths. Thus T_- will prefer to decay to $T_{\pm}$ rather than to $T_{\pm}'$ (k_{-10}) and opening up of the chelate ring becomes a real possibility only under acid conditions. However, under these conditions an alternative process comes into play for the aqua amide (Scheme IV), and the chelated amide is also unreactive.

The promotion of hydrolyzed product by buffers is also readily understandable and Scheme V suggests that this occurs via the acid-catalyzed formation of $T_{\pm}$ or T_+. Thus acetic acid (Figure 5) is more effective than phenol or methyl phosphate at the same pH (stronger acid), and the principle of microscopic reversibility requires that the formation of chelated amide from T (k_{-3}) is not catalyzed by general acids (but see below for HPO_4^{2-}).

The products of the phosphate-catalyzed reactions are also unusual in that some phosphate-promoted loss of water appears to occur in competition with phosphate-catalyzed loss of amine. This result is required by the experiment using $(+)_{589}$-$[Co(en)_2(OH)(glyglyOC_3H_7)]^{2+}$ where some 5% $[Co(en)_2(glyglyOC_3H_7)]^{3+}$ is formed under conditions (0.15 M buffer) where the product distribution has reached a limiting composition (Figure 12). Also, Figure 12 suggests that $H_2PO_4^-$ is better than HPO_4^{2-} at promoting $[Co(en)_2(glyO)]^{2+}$ formation since the maximum yields of hydrolysis product are found under the most acidic conditions consistent with reaction of the hydroxo dipeptide (pH 6-7). Thus acid-catalyzed loss of amine seems to be an important feature of these buffers at least, and it is likely that a transition state of the form ix occurs. Similar transition states have been proposed

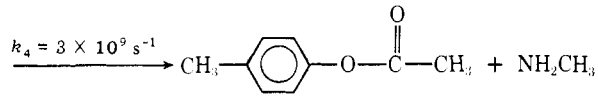

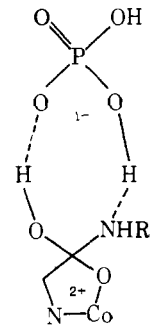

ix

for the phosphate-catalyzed hydrolysis of 4-hydroxybutyranilide.[3] $HMePO_4^-$ likewise markedly promotes the formation of $[Co(en)_2(glyO)]^{2+}$ whereas $MePO_4^{2-}$ is much less discriminating (Figure 5).

Comparison with Related Intramolecular Hydrolysis Reactions. It is appropriate that these metal-catalyzed intramolecular processes be compared with the hydrolysis of 4-hydroxybutyramides and 2-hydroxybenzamides mentioned in the introduction. The following differences are significant.

(1) The rates of reaction over the entire pH range are very much faster having the metal present. Thus the aqua dipeptide hydrolyzes 10^{11} times more rapidly than the dipeptide alone (pH 5), and a factor of 10^7 is involved for the hydroxo dipeptide complex at pH 8. The presence of phosphate enhances the latter reaction considerably so that at pH 8 in 0.1 M buffer the reaction is 10^9 times faster than the same process in the absence of the metal. For the 4-hydroxybutyramide much smaller rate increases were found in the absence of buffers (15-20 at pH $\sim$9 and 800 at pH $\sim$6),[3,7] and the OH^--promoted path for 2-hydroxymethylbenzamide is only 3500 times faster than that for benzamide itself (4×10^{-2} vs. 1.16×10^{-5} M^{-1} s^{-1}, respectively).[4] Phosphate buffers significantly catalyze both reactions but the maximum acceleration found for 4-hydroxybutyramide was only 12 600 at pH 9; under the conditions the buffer-independent cyclization process was held to be rate determining.[3] (2) For the intramolecular reaction of the metal-hydroxo complexes, formation of $Co-O^-$ by prior deprotonation (specific OH^- catalysis) does not occur, but rather deprotonation in the transition state for addition of Co-OH (general base catalysis) occurs. For the similar reaction of 4-hydroxybutyramides, specific OH^- deprotonation of the hydroxyl function is proposed for the OH^--catalyzed reaction at least,[2,3] and general acid/general base promoted loss of amine from the tetrahedral intermediate is considered to be rate determining for all but the highest buffer concentrations.[3,5]

(3) The unusual phosphate dependence on the rate for the metal-hydroxo system (eq 8, Figures 8-11) is interpreted as

resulting from ion pairing in the reactant 3+ aqua complex rather than from a change in rate-determining step as proposed for the organic systems.[3-5]

(4) Opening up of the five-membered metal chelate ring is not competitive with loss of NH_2R or OH^-, whereas it apparently is for the nonmetal systems.[3-5]

Supplementary Material Available: Rate data for the unbuffered reactions of the $[Co(en)_2(OH_2/OH)(glyNHR)]^{1+/2+/3+}$ ions (Table I), rate data for the buffer catalyzed reactions of the *cis*-$[Co(en)_2(OH_2/OH)(glyNH_2)]^{2+/3+}$ ions (Table IV), rate data for the buffer catalyzed reactions of the *cis*-$[Co(en)_2(OH_2/OH)(glyglyOC_3H_7)]^{2+/3+}$ ions (Table V), rate data for the buffer catalyzed reactions of the *cis*-$[Co(en)_2(OH_2/OH)(glyglyO)]^{2+/1+}$ ions (Table VI), rate data for phosphate, carbonate, and arsenate catalyzed reactions of *cis*-$[Co(en)_2(OH)(glyNH_2)]^{2+}$ (Table VIII), rate data for the phosphate catalyzed reaction of *cis*-$[Co(en)_2(OH)(glyglyOC_3H_7)^{2+}$ (Table IX), rate data for hydrolysis of the $[Co(en)_2(glyNHR)]^{3+}$ ions (Table XI), plots of $(k_{obsd} - k_{hyd})$ vs. [buffer] for the reactions of $[Co(en)_2(OH)(glyNH_2)]^{2+}$ (Figure 6), plot of k_{obsd} vs. $[phosphate]_T$ for the cyclization of $[Co(en)_2(OH)(glyglyOC_3H_7)]^{2+}$ as a function of pH (Figure 10), plot of k_{obsd} vs. $[methyl\ phosphate]_T$ for the cyclization of *cis*-$[Co(en)_2(OH)(glyglyOC_3H_7)]^{2+}$ as a function of pH (Figure 11), and repetitive scans during hydrolysis of $[Co(en)_2(glyglyOC_3H_7)](NO_3)_3$ (Figure 13) (18 pages). Ordering information is given on any current masthead page.

References and Notes

(1) C. J. Boreham, D. A. Buckingham, and F. R. Keene, *Inorg. Chem.*, **18**, 28 (1978).
(2) T. C. Bruice and F.-H. Marquardt, *J. Am. Chem. Soc.*, **84**, 365 (1962).
(3) B. A. Cunningham and G. L. Schmir, *J. Am. Chem. Soc.*, **89**, 917 (1967).
(4) (a) C. J. Belke, S. C. K. Su, and J. A. Shafer, *J. Am. Chem. Soc.*, **93**, 4552 (1971); (b) K. N. G. Chiong, S. D. Lewis, and J. A. Shafer, *ibid.*, **97**, 418 (1975).
(5) T. Okuyama and G. L. Schmir, *J. Am. Chem. Soc.*, **94**, 8805 (1972).
(6) G. L. Schmir and B. A. Cunningham, *J. Am. Chem. Soc.*, **87**, 5692 (1965).
(7) B. A. Cunningham and G. L. Schmir, *J. Am. Chem. Soc.*, **88**, 551 (1966).
(8) R. W. Hay and P. J. Morris in "Metal Ions in Biological Systems", Vol. 5, H. Sigel, Ed., Marcel Dekkar, New York, N.Y., 1976, p 173.
(9) D. A. Buckingham in "Biological Aspects of Inorganic Chemistry", Proceedings of the 1976 International Symposium, A. W. Addison, R. W. Cullen, D. Dolphin, and B. R. James, Ed., Wiley-Interscience, New York, N.Y., 1977, p 141.
(10) J. J. Johansen and B. L. Vallee, *Proc. Natl. Acad. Sci. U.S.A.*, **70**, 2006 (1973); *Biochemistry*, **14**, 649 (1975).
(11) R. Breslow and D. Wernick, *Proc. Natl. Acad. Sci. U.S.A.*, **74**, 1303 (1977); *J. Am. Chem. Soc.*, **98**, 259 (1976); E. P. Kang, C. B. Storm, and F. W. Carson, *ibid.*, **97**, 6723 (1975); H. E. Van Wart and B. L. Vallee, *Biochim. Biophys. Acta*, 732 (1977); M. W. Makinen, K. Yamamura, and E. T. Kaiser, *Proc. Natl. Acad. Sci. U.S.A.*, **73**, 3882 (1976).
(12) C. A. Bunton, M. M. Mhala, K. G. Oldham, and C. A. Vernon, *J. Chem. Soc.*, 3293 (1960).
(13) O. Bailly, *C. R. Acad. Sci.*, **170**, 1061 (1920).
(14) C. J. Boreham, Ph.D. Thesis, The Australian National University, July 1978.
(15) D. A. Buckingham, C. E. Davis, D. M. Foster, and A. M. Sargeson, *J. Am. Chem. Soc.*, **92**, 5571 (1970).
(16) P. K. Glasoe and F. A. Long, *J. Phys. Chem.*, **64**, 188 (1960).
(17) Values of k and K_b are based on $pK_w = 13.77$ and $\mu = 1.0$ (KCl): H. S. Harned and W. J. Hamer, *J. Am. Chem. Soc.*, **55**, 2194 (1933). A recent value of pK_w in 1.0 M $NaClO_4$ (13.80) agrees closely with this: R. Fischer and J. Bye, *Bull. Soc. Chim. Fr.*, 2920 (1964). The data for R = H and $CH_2CO_2^-$ is taken largely from ref 15.
(18) Program written by L. M. Engelhardt for a PDP-11 computer.
(19) C. A. Bunton and V. J. Shiner, *J. Am. Chem. Soc.*, **83**, 42 (1961).
(20) C. A. Bunton and V. J. Shiner, *J. Am. Chem. Soc.*, **83**, 3207 (1961).
(21) The second-order rate for alkaline hydrolysis of glycinamide of 2×10^{-3} $M^{-1}\ s^{-1}$ gives $t_{1/2} \simeq 10^{11}$ s at pH 5: H. L. Conley and R. B. Martin, *J. Phys. Chem.*, **69**, 2923 (1965).
(22) The observation that removal of coordinated water competes for the intramolecular process requires the former reaction to also be fast, $k_{obsd} \sim 10^{-2}\ s^{-1}$ at 25 °C, $\mu = 1.0$ ($NaClO_4$).
(23) F. Basolo and G. S. Hammaker, *Inorg. Chem.*, 1, 1 (1962).
(24) G. Basza and H. Diebler, *Proc. Int. Conf. Coord. Chem.*, **15**, 442 (1973).
(25) R. K. Wharton, R. S. Taylor, and A. G. Sykes, *Inorg. Chem.*, **14**, 33 (1975).
(26) T. A. Beech, N. C. Lawrence, and S. F. Lincoln, *Aust. J. Chem.*, **26**, 1988 (1973).
(27) R. K. Murmann and H. Taube, *J. Am. Chem. Soc.*, **78**, 4886 (1956).
(28) J. C. Sullivan and J. E. French, *Inorg. Chem.*, **3**, 832 (1964).
(29) A. D. Fowles and D. R. Stranks, *Inorg. Chem.*, **6**, 1267 (1967).
(30) These reactions are somewhat different, however, as the oxy anions themselves undergo rapid oxygen exchange in water.
(31) W. P. Jencks, *J. Am. Chem. Soc.*, **94**, 4731 (1972).
(32) W. P. Jencks, *Chem. Rev.*, **72**, 705 (1972).
(33) An estimated pK_a of -4 for the protonated amide residues gives a specific rate of $10^8\ s^{-1}$ for this species (R = H).
(34) W. P. Jencks in "Catalysis in Chemistry and Enzymology", McGraw-Hill, New York, N.Y., 1969, Chapter 4.
(35) F. A. Posey and H. Taube, *J. Am. Chem. Soc.*, **78**, 15 (1956).
(36) D. A. Buckingham, D. M. Foster, and A. M. Sargeson, *J. Am. Chem. Soc.*, **92**, 6151 (1970).
(37) D. A. Buckingham, I. I. Olsen, and A. M. Sargeson, *J. Am. Chem. Soc.*, **90**, 6654 (1968).
(38) The ^{18}O tracer result of the hydroxyglycinamide reaction is contained in ref 36. Under the conditions reported there, sufficient time was allowed following base hydrolysis of *cis*-$[Co(en)_2Br(glyNH_2)]^{2+}$ in $H_2\ ^{18}O$ to allow a large proportion of the hydroxo amide to react, and the subsequent product shows that this part retains the ^{18}O label in the chelate ring of the hydrolyzed glycinate fragment.
(39) D. A. Buckingham, D. M. Foster, and A. M. Sargeson, *J. Am. Chem. Soc.*, **91**, 3451 (1969).
(40) D. A. Buckingham, J. Dekkers, and A. M. Sargeson, *J. Am. Chem. Soc.*, **95**, 4173 (1973).
(41) E. Baraniak, Ph.D. Thesis, The Australian National University, March 1973.
(42) J. Bjerrum, *Adv. Chem. Ser.*, **No. 62**, 178 (1967).
(43) The pK_as for T, T_+, and $T_\pm$ given in Scheme VII were estimated using the method and data of Fox and Jencks[44] and others,[47] assuming that Co^{3+} attached to the phenolic oxygen of the tetrahedral intermediate has an intermediate effect to that of H^+. Thus from a $pK_a = 8.0$ for $CH_3NH_2^+CH_2CO_2Et$, that for $CH_3C(OH)_2NH_2^+CH_2CO_2Et$ and $CH_3C(OH)(O^-)NH_2^+CH_2CO_2Et$ are estimated at 4.1 and 8.9, respectively, giving a pK_a value of 6.5 for $CH_3C(OH)(OCo^{3+})^+NH_2CH_2CO_2Et$. Similarly[47] the pK_a for the alcohol function in $CH_3C(OH)(OCo^{3+})(NHCH_2CO_2Et)$ was estimated at 13.0. This intermediate polarizing ability of Co^{3+} when two atoms removed from the acidic center has been observed many times previously.[9] The influence of the Co^{3+} moiety on the aminomethyl function of the five-membered chelate was allowed for using data for $CH_3NH_3^+$ (10.7), $NH_2CH_2CH_2NH_3^+$ (9.0), and $(en)_2(Br)Co{-}NH_2CH_2CH_2NH_3^+$ (7.3). The Co^{3+} function has a similar property to H^+ when three atoms removed from the acidic center (viz., $CoNH_2CH_2CH_2NH_3^+$ (6.8)) and this also appears to be a common property (viz., $(NH_3)_5Co^{3+}NH_2CH_2CO_2H$ (2.3), $NH_3^+CH_2CO_2H$ (2.3) carboxylic acid functionality). Adjusting the above estimates for the tetrahedral species for this effect ~3 pK_a units) gives $pK_T \sim 10$, $pK_{T_+} \sim 3.5$, and following Jencks and Satterthwait's estimates for the related ionization[45] gives $pK_{T_\pm} \sim 8.5$ and $pK_{T_+} \sim 5$.
(44) J. P. Fox and W. P. Jencks, *J. Am. Chem. Soc.*, **96**, 1436 (1974).
(45) A. C. Satterthwait and W. P. Jencks, *J. Am. Chem. Soc.*, **96**, 7031 (1974).
(46) D. A. Buckingham, P. J. Morris, A. M. Sargeson, and A. Zanella, *Inorg. Chem.*, **16**, 1910 (1977).
(47) M. F. Aldersley, A. J. Kirby, P. W. Lancaster, R. S. McDonald, and C. R. Smith, *J. Chem. Soc., Perkin Trans. 2*, 1498 (1974).
(48) W. F. K. Wynn-Jones, *Trans. Faraday Soc.*, **32**, 1397 (1936).